

## Article

# Spatial Distribution and Hydrogeochemical Factors Influencing the Occurrence of Total Coliform and *E. coli* Bacteria in Groundwater in a Hyperarid Area, Ad-Dawadmi, Saudi Arabia

Hassan E. Gomaa<sup>1,2,3,\*</sup> , Mohamed Charni<sup>4,5</sup> , AbdAllah A. Alotibi<sup>1,3</sup> , Abdulhadi H. AlMarri<sup>6</sup> and Fatma A. Gomaa<sup>1,7,\*</sup>

- <sup>1</sup> Department of Chemistry, College of Science and Humanities at Ad-Dawadmi, Shaqra University, Ad-Dawadmi 11911, Saudi Arabia
  - <sup>2</sup> Department of Nuclear Safety Engineering, Nuclear Installations Safety Division, Atomic Energy Authority, Nasr City 11765, Egypt
  - <sup>3</sup> Water Research Group, College of Science and Humanities at Ad-Dawadmi, Shaqra University, Ad-Dawadmi 11911, Saudi Arabia
  - <sup>4</sup> Department of Biology, College of Science and Humanities at Ad-Dawadmi, Shaqra University, Ad-Dawadmi 11911, Saudi Arabia
  - <sup>5</sup> Laboratory of Biodiversity, Parasitology, and Ecology of Aquatic Ecosystems LR18ES05, Faculty of Sciences of Tunis, University of Tunis El Manar, Tunis 2092, Tunisia
  - <sup>6</sup> Department of Chemistry, University College-Alwajh, University of Tabuk, Tabuk 71421, Saudi Arabia
  - <sup>7</sup> Department of Chemistry, College of Women for Science, Arts, and Education, Ain Shams University, Cairo 11757, Egypt
- \* Correspondence: [hjomaah@su.edu.sa](mailto:hjomaah@su.edu.sa) or [hassan\\_emgh@yahoo.com](mailto:hassan_emgh@yahoo.com) (H.E.G.); [fjomaah@su.edu.sa](mailto:fjomaah@su.edu.sa) or [fatma\\_emgh@yahoo.com](mailto:fatma_emgh@yahoo.com) (F.A.G.)



**Citation:** Gomaa, H.E.; Charni, M.; Alotibi, A.A.; AlMarri, A.H.; Gomaa, F.A. Spatial Distribution and Hydrogeochemical Factors Influencing the Occurrence of Total Coliform and *E. coli* Bacteria in Groundwater in a Hyperarid Area, Ad-Dawadmi, Saudi Arabia. *Water* **2022**, *14*, 3471. <https://doi.org/10.3390/w14213471>

Academic Editor: Yuanzheng Zhai

Received: 10 October 2022

Accepted: 26 October 2022

Published: 30 October 2022

**Publisher's Note:** MDPI stays neutral with regard to jurisdictional claims in published maps and institutional affiliations.



**Copyright:** © 2022 by the authors. Licensee MDPI, Basel, Switzerland. This article is an open access article distributed under the terms and conditions of the Creative Commons Attribution (CC BY) license (<https://creativecommons.org/licenses/by/4.0/>).

**Abstract:** Coliforms (FB) posing population health risks in groundwater (GW) have been identified for decades, with recent studies assessing how hydrogeological and non-hydrogeological parameters correlate with their presence. This study focused on explaining the physicochemical and hydrological factors influencing the presence of fecal contamination in the GW system of Ad-Dawadmi, KSA, a hyperarid area facing a prolonged drought. It was designed and implemented by sampling 47 working wells and their laboratory analysis. The data analyses indicated that the salinity exhibited a purification effect such that at levels higher than 3500 and 6000 mg/L, no *E. coli* and total coliform (TC) were detected. Heavy metals, especially copper, showed strong, hygienic effects at 195 and 300 µg/L thresholds for *E. coli* and TC, respectively, while those of Fe were at 1200 and 2000 µg/L. Nitrates, dissolved organic carbon (DOC), and dissolved oxygen (DO) showed a quasi-random interrelationship with FB. The occurrence of FB in boreholes up to 52 m below ground level (BGL) challenges the single water resource in the region. Integrating various analyses help constrain and provide multiple lines of evidence for the inferred remarks. This work presented some methodological aspects for understanding the effects of the physicochemical and hydrogeological factors on FB that may better protect water quality and improve human health outcomes.

**Keywords:** groundwater; *E. coli*; total coliform; spatial distribution; urbanization; hyperarid; Ad-Dawadmi; Saudi Arabia

## 1. Introduction

Water is an indispensable resource for human life and related activities. With the increase in the world's population, industrialization, reclamation, agriculture, livestock farming, and urbanization, the water demands are even more significant, accompanied by the deterioration of essential water sources worldwide [1]. The importance of water geochemical studies is recognizing and understanding the hydrogeochemical and biophysicochemical processes and factors controlling the groundwater (GW) characteristics

and identifying the deterioration pathways [2,3]. Undoubtedly, natural conditions and anthropogenic activities impact the groundwater's physicochemical, biological, and quality characteristics. The natural conditions include climate, geomorphology, geology (mineralogy and sedimentology of the containing rocks), and hydrogeological factors. The anthropogenic activities introduce additional stresses related to reclamation, cultivation, urbanization, industrialization, and livestock ranching [4–6]. Once the contaminants enter the subsurface environment, they may take several years to have vanished, becoming dispersed over broad areas of the aquifer and rendering GW supplies unsuitable for different uses [7–10]. The microbial quality of GW has been threatened by contamination with untreated domestic wastewater, animal manure, and other industrial discharges [11]. Because bacteria can remain alive for a long time, population health risks arise. The occurrence of coliform bacteria, also called fecal bacteria (FB), in water exceeding the recommended limit for domestic uses and irrigation of raw-eaten crops has a significant role in the prevalence of diverse diseases causing endemic and epidemic outbreaks worldwide [12,13]. It was reported that infections by waterborne diseases are over 250 million per year, with about ten to twenty million dying [14,15]. Furthermore, it was reported that about 30,000 mortalities per day occur in developing countries due to unsanitized water consumption [12,16].

The potential sources of fecal bacteria and/or pathogens include humans, wildlife, rodents, and domestic livestock. The contamination indicator bacteria, total coliform (TC), and *Escherichia coli* (*E. coli*), have been employed as sanitary indicators for evaluating GW impacted by feces. Public health authorities consider that these indicators are associated with organisms causing significant concern in developing and developed countries [17]. The detection of such indicator bacteria in the GW suggests the existence of a route of contamination, such as pit latrine, landfill, surface water interconnection, septic source, or livestock manures. Thus, pathogenic bacteria can utilize such a pathway, colonizing the water used as a supply [7], necessitating their appropriate management as they can directly or indirectly impact human health [18], causing mild illness, while others may lead to severe waterborne diseases [19]. The feces of sick persons in water supplies causes common symptoms, especially in children and elderly household members, such as gastrointestinal upset, cholera, typhoid fever, dysentery and gastroenteritis fever, abdominal cramps, and diarrhea [18–21]. Detecting such pollution indicator bacteria has become the routine microbiological test of water quality adopted by many public health officers to prevent the further spreading of pathogens. The drinking water standards require that the TC, and *E. coli* bacteria be absent [16,22,23].

Despite GW being supposed to be bacterial pathogens-free, recent demonstrations many decades ago detected such bacteria in a substantial fraction of GW sources [13–15]. Some factors can influence the presence and quantity of coliform bacteria in GW, such as weather conditions, time of year, and human activities (agricultural, farming, livestock ranching, etc.) [18–21].

The transport of GW in shallow aquifers is essentially dependent on the climate conditions and the hydrogeological settings [2,24–27]. The aquifer sediment, type and characteristics of the subsurface soil, the microbial population, the physical state of microbes (alive or dead), and the hydrological conditions, such as water temperature and quality, are all influential parameters on the transport, rate of survival, and fate of microbes in the subsurface [12,28–30]. To control soil and GW pollution, the mechanisms of bacterial fate (attenuation) and transport in the subsurface should be understood [28,31–34]. Understanding the vadose zone's role in fecal coliform flow and transport through the soil until reaching the shallow water table is of utmost importance [32,35,36]. Several studies tried to investigate the interrelationships between the temporal variability of *E. coli* and the wells' depths, seasonal rainfall characteristics, population density, and the distance to septic tanks [18,32,36–39].

Several qualitative and quantitative factors have been statistically analyzed, including geological, hydrological, sanitary risk factors, geochemical, well types, and maintenance variables [12,36,40,41].

Different methodologies have been followed, such as a statistical principal component analysis (PCA), enabling the inclusion of an interdisciplinary set of variables to get information on the correlations between the numerous variables, usually partitioned in the analysis [38,42,43], nested binary logistic models, and multivariate regression models [12], taxonomy-based and binary correlation [7,44–46], experimentally controlled assessments [47,48], and spatial distribution (SD), sources tracking and identification [7,11,45,46,49–52]. In addition, studies that discriminated and quantified how the hydrogeological, physicochemical, and quality factors correlate with the occurrence of *E. coli* to be used as an indicator (proxy) of fecal contamination have been conducted [33,34,53]. Other works aimed to develop microbial pollution indices [20]. The stresses and effects of the environmental factors and heavy metals concentrations on the microbial community in groundwater systems were also demonstrated [12,14,21,54–56]. The factors identified as the playmakers contributing to the problem are precipitation, livestock farming, pit latrines, landfills construction and casing, wells construction, water table hydrodynamics, and installment of wastewater treatment plants and the adequacy of treatment and discharges.

Several researchers have investigated that Gram-negative bacteria (FB) are more tolerant than Gram-positive to heavy metals concluding that copper affected the microbial community, while Zn, Ni, Fe, and Cd were uncorrelated with the soil's microbial contents [57,58]. Furthermore, some demonstrations concluded that the tolerability of fecal bacteria to specific levels of heavy metals under natural conditions might differ. The fungi and bacteria were in antagonistic relationships in different ecosystems that the activity increase of one group of organisms may decrease the activity of the other group, i.e., high microbial counts had lower fungi counts and vice versa. The soil microbes' ascending order resistance to the trace metals' toxicity is Gram-positive bacteria, Gram-negative bacteria, and fungi [59–61]. A recent exciting study pointed out the possible occurrence of environmental adaptation that makes just identifying fecal bacteria an overestimation to be the sole fingerprint of fecal contamination, which is the base of its regulatory adoption [31].

Howard et al. concluded that there is no significant relationship between fecal contamination and the wells' proximity to pit latrines, pointing out that many variables influence the occurrence of thermotolerant in shallow GW [37]. Although the geological formation was not directly related to fecal contamination, some hydrogeological and physicochemical factors (redox condition, flow velocity, water column, etc.) were significant [34,42,43]. Moreover, Ferrer et al. stated that the geochemical elements and GW depth could be facile indicators of fecal bacteria enabling their possible usage as a proxy for fecal contamination [42]. Including all such variables as interplaying factors complexed the situation contributing to large uncertainty budgets to the conclusions. Moreover, selecting readily measurable parameters as surrogates due to the longer time needed for microbial assessments may lead to erroneous estimations due to selecting weakly related or un-interrelated parameters.

This work focused on delineating the most significant physicochemical, hydrological, and geochemical factors influencing the presence of fecal contamination in the GW system of Ad-Dawadmi, KSA, a hyperarid area facing a climatic change of prolonged drought. Moreover, the study aimed to examine the relationships between explanatory (surrogate) variables and FB and prioritize the most reliable physicochemical parameters showing prominent and consistent correlations with the presence of FB to be used as surrogate variables in bacterial contamination predicting models in hyperarid regions. The study's design followed a graded approach starting by characterizing the current status of the GW system under study based on the laboratory analyses results of the collected samples using descriptive statistics and spatial distribution maps. The second stage involved the investigation of the binary effects (i.e., effects of two factors at a time on the response parameter (fecal bacteria presence) using the box plot matrix. Then, moving on with studying the most prominent influential parameters using ternary effects tools (bubbles diagrams and 3D surface plots) to help double constrain and provide multiple lines of evidence to figure out the factors that have a hygienic role (bacterial purification) and the capacity of such effects when combined.

## 2. Materials and Methods

### 2.1. Description of the Study Area

The study area (Ad-Dawadmi metropolitan and its nearby environs) represents the central part of the Ad-Dawadmi governorate, northwest of Riyadh Province, KSA, Figure 1. Ad-Dawadmi governorate is bordered on the east by Shaqra governorate and the Marat Center, on the west by Afif Governorate, northwest by Rass governorate, and on the north by Unaizah Governorate, Al-Mithnab, Al -Bukayriyah, and be part of the administrative area of the Buraidah city and from the south by the Governorate of Al-Quwaiyah. It is about 250 km west of Riyadh [62]. It ranks 5th in the governorates of the region with an area of  $\approx 27,500$  km<sup>2</sup>, a population of 217,305 people, and 43,121 houses [63]. Its western half lies at the most eastern fringe of the so-called Arabian Shield. Although the governorate is generally extroverted, there are many distributed rocky outcrops and plateaus, with the highest 1307 m (Jabal Al-Nir in the far west) and the lowest plain 660 m in the far northeast with a mean elevation of 940 m above sea level. The surface generally slopes towards the east and northeast, where most valleys tend to be east and northeast [62]. The shallow sedimentary thickness ranges from 1.0 m and 7.0 m, overlying the bedrock generally slopes from the west to the east [64]. Many large and small wadis and large valleys include Al-Rasha valley, Wadi Khnuqa, Jaham valley, the valley of the Dogs, Tasrir valley, Haysha valley, and wadi Abu Ashr. In addition to many small reefs and valleys like Shoaib Abu Ashira, Shoaib Wasit, Shoaib Hamror, Shoaib wayward, Shoaib Al-Haid, Shoaib Awada, Shoaib Al Rafaia, Shoaib Qubeia, Shoaib Jaham, Shoaib or Alanda, and Shoaib Dawadmi. Ad-Dawadmi is famous for growing various crops and witnessing remarkable agricultural development in the past thirty years. It is still fortunate to maintain its production levels [65]. Moreover, livestock farming (primarily camels, goats, and sheep), poultry farms, and aquaculture are widely spread over the governorate [62]. The Ad-Dawadmi governorate lies at the Arabian Shield outer eastern-central border with unconformably overlying Palaeozoic sediments in the central KSA high pediment containing Precambrian granitic rocks complex and two belts of folded metasediments and two oval layered basic complexes. The conformable calcareous Ar-Ridaniyah, arenaceous, and semipelitic Abt formations are the oldest rocks deposited in a transgressive subsiding likely marine environment during the Precambrian [66–68].

The Ad-Dawadmi climate is generally hyperarid with minimal precipitation, long consecutive drought periods, and remarkable effects of climatic change. This is the fifth consecutive year with nearly no precipitation except for accidental short showers. The long-term yearly average is only 4.9 mm from 2005 to 2015, with temperatures 8–42 °C for the hot and cold periods, respectively [69]. Groundwater, the artery of life ecologically and sustainably, is the sole available water resource since precipitation is very limited in duration and recently in amounts. However, characterization, monitoring, and studying of the cause-and-effect relationship for the aquifer in the region are scarce and not conducted. The study region is the central part of the governorate, namely the Ad-Dawadmi metropolitan and its nearby environs (latitudes 24°20' to 24°40' N and longitudes 44°12' to 44°33' E).

The self-consumption and ranching of livestock are widespread throughout the area. A wastewater treatment plant serves the central metropolitan and pit latrines as sanitation facilities throughout the rural areas. The two types of groundwater wells in the area are (1) less abundant hand-dug wells of a large diameter, up to 40 m deep, equipped with submersible pumps of different powers and mostly uncovered, and (2) predominant deep boreholes with small diameter, with different depths from 26 to 52 m. The water table levels were consistently in the range of a few meters, 2–3, and even less below ground level (BGL) in 1996 [64]. These levels declined sharply and are consistently more than 12 m BGL.

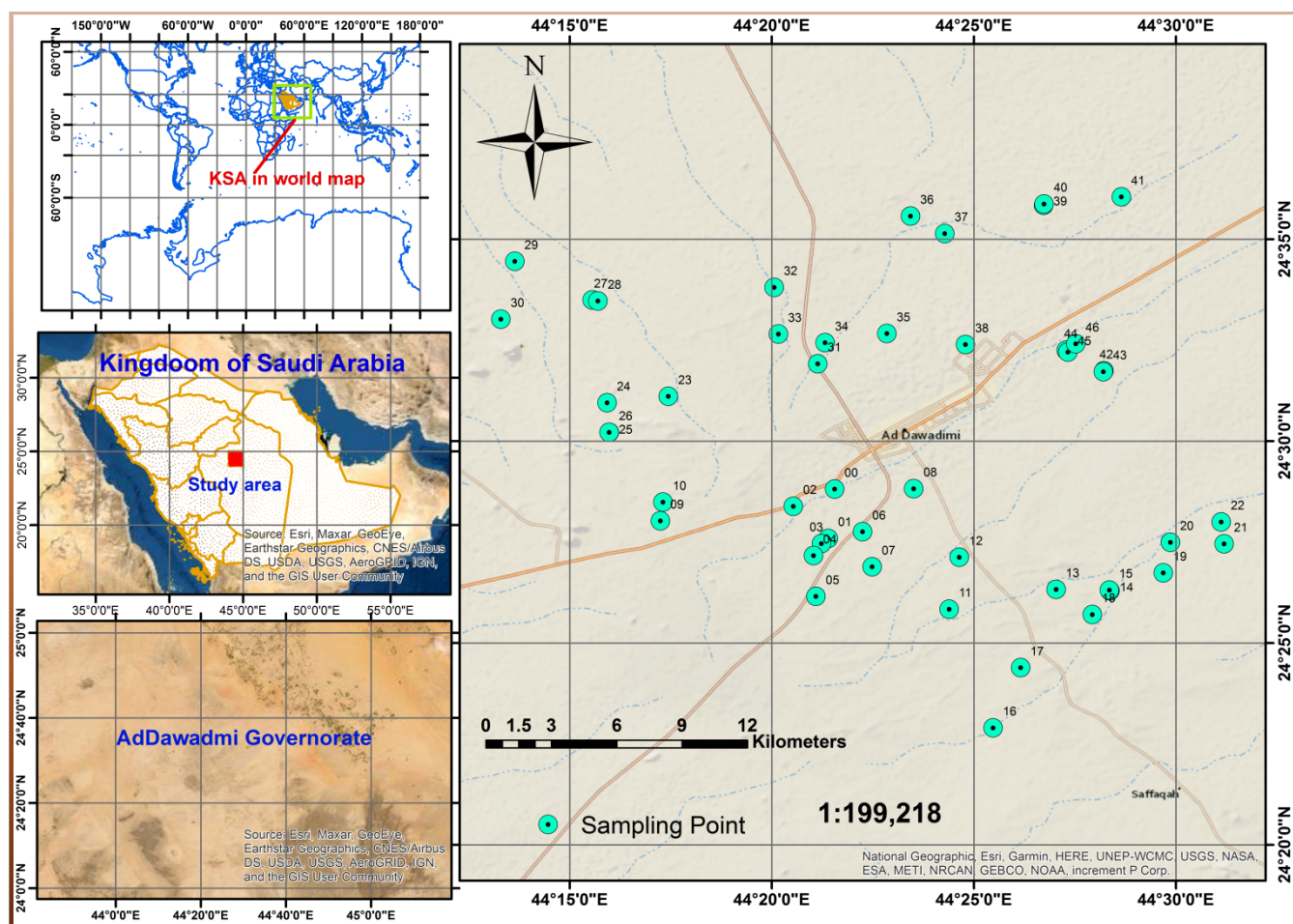


Figure 1. Study area location and the sampling points spatial distribution.

## 2.2. Sampling and Preservation

The sampling protocols, the analytical methods and procedures, the instrumental techniques, and data management and analyses used, adopted, adapted, and followed throughout the different phases of this work to fulfill the ultimate goals are described in the forthcoming section. In five sampling campaigns, 47 water samples were collected from accessible and active wells after pumping enough to ensure that representative aquifers' water is being attained and thus reflecting the chemistry of the groundwater with the least possible uncertainty [70]. Separate acid-cleaned 1 L polypropylene bottles were carefully rinsed several times with the well water before sampling. The bottles were filled, preserved, and cooled as per the different measurands (analytes) rules. The respective precautions and rules were taken into consideration with commensurate care, preservation, immediate pretreatments, and in-field measurements. The sampling points' location and distribution are shown in Figure 1. Samples collected for the hydrochemical (major cations and anions) and bacteriological analyses were chilled with no preservatives added. Once back at the laboratory (Water and Environment Research Unit (WERU), College of Science and Humanities at Ad-Dawadmi, Shaqra University), they were split and pretreated as per the procedures of the different individual analyses according to the standard methods and sampling directions [71–73]. To stop bacterial growth and block oxidation reactions, samples collected to measure ammonium and nitrate were preserved by acidification with concentrated sulfuric acid to  $\text{pH} \approx 2$ . Samples for measuring *T. coliform* and *E. coli* were collected in cleaned 250 mL bottles, were chilled in an icebox in the field until returned to the laboratory, and processed on the same sampling day. Samples for trace elements analysis (100 mL) were chilled in an icebox until going back to the laboratory within 6–8 h. Then,

samples were filtered using a 0.45 µm cellulose acetate filter paper to remove suspended sediments before acidification with ≈0.25 mL concentrated trace elements analysis grade nitric acid to stop bacterial growth, block oxidation reactions, and prevent precipitation of targeted constituents.

### 2.3. Analyses and Procedures

#### 2.3.1. In-Field Parameters

The electrical conductivity (EC) was measured using ThermoScientific, Texas ORION STAR A122 electrical conductivity meter. The meter's calibration and occasional operational checks have been carried out before and during the sampling campaign. The pH, the power of hydrogen ion, was recorded using a PascoScientific, California pH electrode connected to an Explorer GLX, Pasco data logger via PASPort CHEMISTRY Sensor, PascoScientific. In addition, temperature (T) was measured using an independent electrode connected to the data logger through the Passport CHEMISTRY Sensor head. DISSOLVED OXYGEN meter, Pasco Scientific electrode was used for measuring dissolved oxygen (DO) levels in mg/L. All meters were calibrated, stored, and maintained following the manufacturer's instructions.

#### 2.3.2. Hydrochemical Characterization

##### a. Nitrate and Ammonium

The phenol sulphonic acid method [74] was modified, refined, and further tuned to measure nitrate ( $\text{NO}_3^-$ ) ion concentration at 410 nm wavelength. The modification involved the addition of 25 mL of 6N  $\text{NH}_4\text{OH}$  in the color production complexing step instead of the initially reported 3N ammonia water. The modified ammonia diffusion method [75] was adopted and followed to measure ammonium ( $\text{NH}_4^+$ ) ion concentration. Rising pH to ≈11 using sodium hydroxide solution converts dissolved ( $\text{NH}_4^+$ ) to ammonia ( $\text{NH}_3$ ) gas with a lower solubility and explores a stripping tendency out of the solution. The stripped ( $\text{NH}_3$ ) gas is collected into an acid trap constructed by placing 5 mL of 0.05N  $\text{H}_2\text{SO}_4$  in a polypropylene cap covered with a small piece of Teflon membrane. The samples bottles containing the acid traps were closed tightly and incubated for five days at room temperature and shaking amplitude 180 rpm. At the end of the incubation period, the contents of the acid caps were washed and diluted to 100 mL, Nessler's reagent added to a small portion of those samples, and the intensity of the resulting yellow color was measured spectrophotometrically at 405 nm wavelength.

##### b. Dissolved Organic Carbon (DOC)

DOC was quantified spectrophotometrically using JENWAY 6850 UV/Vis. Spectrophotometer at 254 nm wavelength. The quantification was achieved by constructing the respective calibration curve using potassium hydrogen phthalate (PHP) as a DOC proxy that assured a linear relationship between absorbance and concentration, with  $R^2$  consistently higher than 0.99.

##### c. Coliform detection

According to the manufacturer's procedure, bacteriological detection of TC and *E. coli* bacteria were conducted using EC blue 100 p screening medium [76]. EC blue is a simple, reliable technique that enables the rapid, confirmed detection of the TC and the pathogenic *E. coli*. It is a pre-dispensed dry blended reagent formulation designed to detect and confirm *E. coli* and TC. One EC blue sachet is added to 100 mL of the examined water. After 10 s of swirling, the container is incubated at 37 °C for 24 h. The presence (positive) of *T. coilf.* is indicated by the color change to green or blue within 24 h or less due to splitting the chromogenic substrate (X-Gal) in the EC Blue Broth. No color change in the mix indicates coliform's absence (negative). Positive samples are then exposed to a UV light source providing a monochromatic beam of 365 nm wavelength to check the *E. coli* presence. *E. coli* is distinguished from others by its ability to fluoresce in the fluorogenic substrate (MUG), which the beta-glucuronidase enzyme will split, yielding a blue fluorescence under UV light [76–78].

#### d. Trace Elements Analysis

The targeted elements; iron, lead, manganese, cobalt, and copper, were quantified employing the atomic absorption technique using SensAA<sub>DUAL</sub>, GBC Scientific Equipment atomic absorption spectrometer using acetylene-air as the fuel-oxidizer mix. The manufacturer's procedures and operational directions were followed precisely. The relevant quality control and quality assurance procedures have been adhered to.

#### 2.4. Geospatial and Geostatistical Analyses

The spatial analysis tools, including interpolations and overlays of ArcGIS 10.8 software, were used to analyze, map, and aggregate the GW chemical, microbiological, and physical parameters. Minitab<sup>®</sup>18 statistical package was used to execute the statistical analyses and construct the 3D surface plots.

### 3. Results and Discussion

#### 3.1. Physicochemical and Microbiological, Properties

Table 1 summarizes the descriptive statistics of the physicochemical, and microbiological properties. The mean temperature is 27.32 °C with a standard deviation (sd)  $\pm$  2.168, n = 47, ranging from 21.5 °C to 31.8 °C. The tiny sd value hints at the recharge occurring with no significant temperature variability from one locality to another since the variabilities are related to the recharge with rainfall that deeper groundwater has a higher temperature than the shallow ones [79]. Nevertheless, the range of  $\approx$ 10 °C indicates that extremes were causing this range to widen, slightly affecting the main central tendency. The temperature has no predefined limits in regulations for drinking water or irrigation. However, it significantly affects the GW weathering and various interactions with the hosting rocks.

**Table 1.** Descriptive statistics summary of the concerned measured parameters in the groundwater samples.

Variable	Mean	SE Mean	sd	Coef. Var.	Min.	Q1	Median	Q3	Maximum	Range	IQR	Skewness	Kurtosis
Temp, °C	27.32	0.32	2.17	7.94	21.50	25.00	27.50	29.00	31.80	10.30	4.00	−0.10	−0.13
pH	7.34	0.05	0.35	4.71	6.80	7.10	7.33	7.54	8.35	1.55	0.44	0.64	0.37
TDS, mg/L	3293.00	344.00	2359.00	71.65	161.00	1852.00	2696.00	4442.00	11,334.00	11,173.00	2590.00	1.39	2.18
DO, mg/L	11.88	0.28	1.88	15.85	7.00	10.40	12.40	13.20	14.50	7.50	2.80	−0.78	−0.22
DOC, mg/L	1.89	0.21	1.43	75.28	0.13	0.89	1.48	2.55	7.65	7.52	1.66	1.82	4.80
TC	0.51	0.07	0.51	98.95	0.00	0.00	1.00	1.00	1.00	1.00	1.00	−0.04	−2.09
<i>E. coli</i>	0.19	0.06	0.39	207.70	0.00	0.00	0.00	0.00	1.00	1.00	0.00	1.62	0.65
NH <sub>4</sub> , mg/L	0.024	0.005	0.04	150.10	0.00	0.00	0.007	0.04	0.18	0.18	0.04	2.44	7.49
NO <sub>3</sub> , mg/L	72.70	9.87	67.67	93.09	0.21	28.94	51.24	116.53	269.28	269.07	87.59	1.48	1.80
Cu µg/L	67.60	19.40	132.80	196.42	0.00	0.00	0.00	93.80	583.30	583.30	93.80	2.23	4.71
Pb µg/L	300.90	36.00	246.80	82.02	0.00	0.00	304.70	444.20	852.90	852.90	444.20	0.31	−0.90
Mn µg/L	338.50	30.90	211.50	62.48	20.00	160.00	300.00	500.00	800.00	780.00	340.00	0.51	−0.81
Co µg/L	98.90	29.00	198.50	200.74	0.00	0.00	0.00	41.10	684.90	684.90	41.10	2.03	3.12
Fe µg/L	942.90	81.20	556.70	59.04	100.00	543.50	880.00	1152.20	3000.00	2900.00	608.70	1.46	3.32
WD, m BGL	38.43	1.21	8.28	21.54	25.00	30.00	40.00	45.00	52.00	27.00	15.00	0.03	−1.09

Notes: Number of samples n = 47, sd: standard deviation, Q1: first Quartile; WD: Well Depth; BGL: Below ground level, IQR: inter Quartile Range.

TDS showed a significant spread over a range of 11,173 from 161 to 11,334 mg/L with a mean of 3293 and sd  $\pm$  2359. The immense value of sd indicates the presence of a significant portion of the samples with extreme TDS values. The significant values of Skewness and Kurtosis demonstrate the effects of those extremes that nullify the normal distribution hypothesis. pH is one of the most important operational water quality param-

ters widely measured for GW, providing preliminary information about the geochemical equilibrium [80,81]. The pH values were spread over a narrow span with an average of 7.33 and  $sd \pm 0.345$ ,  $n = 47$ , ranging from 6.8 to 8.35. The pH almost has no direct threat to the consumers, and it is considered an aesthetic quality parameter of water. Extreme pH values can result from accidental spills and seepages, acid rains, and types of weathered rocks. Nevertheless, it is not legally binding under EPA regulations [82].

However, the pH has a predefined limit in regulations for drinking water or irrigation from 6.5 to 8.5 [83,84], while that recommended by “The Technical Gulf Committee for Food and Agricultural Product Standards” is 6.5 to 8 [85]. The pH profoundly affects the proliferation of TC and *E. coli*. Microorganisms have pH limits below which they will not grow, with most preferring the neutral pH for optimum growth [86]. The degree of acidity is crucial in the growth of Gram-negative bacteria, including coliform bacteria and *E. coli*, which grow best at a near-neutral pH of 6–8. [12,87,88]. The results show that pH distribution patterns in the study site were 6.9–8.3, enveloping the suitable range of bacteria survival.

Dissolved oxygen (DO) levels were consistently high, with few exceptions demonstrating lowered levels rejecting the normal distribution hypothesis at  $p < 0.005$  according to the Anderson–Darling test [89]. DO central tendency quantifiers yield close values, 11.877 and 12.4 for the mean and median, respectively, emphasizing that the dataset is extremes-free. Moreover, the DO range is 7.5 mg/L from 7 to 14.5 mg/L, with the first quartile (Q1) at 10.4 and the third quartile (Q3) at 13.2. The slight negative Skewness and Kurtosis values are due to the dataset shift towards the upper limit, indicating that most samples have higher DO contents.

Nitrogenous ions,  $NH_4^+$  and  $NO_3^-$ , showed different distributions.  $NH_4^+$  contents were consistently very low, as expected for groundwater. In contrast,  $NO_3^-$  showed large variabilities ranging from 0.21 to 270 mg/L with  $sd \pm 67.67$ . The higher positive values of Skewness and Kurtosis mean that the median shifted toward the lower values, indicating the occurrence of extremes at some localities as corroborated by rejecting the normal distribution hypothesis at  $p < 0.005$  by the Anderson–Darling test.

The trace elements’ ranges and distribution have differed from one element to another, as shown in the box plot in Figure 2. Boxplot is suited to assess and compare sample distributions’ shape, central tendency, and variability and look for outliers showing, by default, each group’s median, interquartile range, range, and outliers [90]. As shown, the concentrations of the elements are in ascending order,  $Cu < Co < Mn < Pb < Fe$ . All elements are not normally distributed, with the Mn and Pb having the lower Skewness and Kurtosis values. This trend seems logical since the other elements occurred in certain localities only, with many sampling points giving Zero values except Fe, which may be due to extremes at particular locations, although distributed all over the entire area.

Total coliform was assessed qualitatively as present (+) or absent (–). These categorical parameters are replaced to facilitate manipulation with 0 for (–) and 1 for (+). Therefore, the mean represents the fraction of positive samples in the data set. Table (1) shows that the mean is 0.5016, indicating that 50% of the samples were contaminated with TC. Similarly, *E. coli*’s mean is 0.1915, i.e.,  $\approx 20\%$  or one-fifth of the samples are positive for *E. coli*. Intuitively, all samples that were positive for *E. coli* were positive for TC, while the reverse was not true.

### 3.2. Spatial Distribution of the Measured Parameters

The spatial distribution (SD) maps of the concerned parameters are interpolated using ArcGIS 10.8 software in order to draw site-specific conclusions and explanations. The inverse distance weighting (IDW) interpolation algorithm was chosen as it claims to retain viewing the data-intrinsic heterogeneities. In the following SD maps, the algorithm, the color, and the interpolation parameters are the same to help contrast the similarities and differences in the spatial distribution of the concerned parameters. Figure 3 presents the SD of TC, *E. coli*, pH, Temp., DO, TDS, Cu, Co, Pb, Mn, Fe, DOC, and well depth (WD).

The philosophy behind portraying the spatial distribution of all such parameters is to look for the intraindividual distributions' similarities and dissimilarities with the criteria that similar distribution trends with TC and *E. coli* are considered positive relationships and vice versa. This philosophy is deemed helpful since the study area experience evenly distributed human activities, including livestock farming and the potential FB sources. Keeping this in mind, the similarities and dissimilarities reflected in the spatial distributions may demarcate the effects of the physicochemical and hydrogeological (site-specific) parameters on the FB presence.

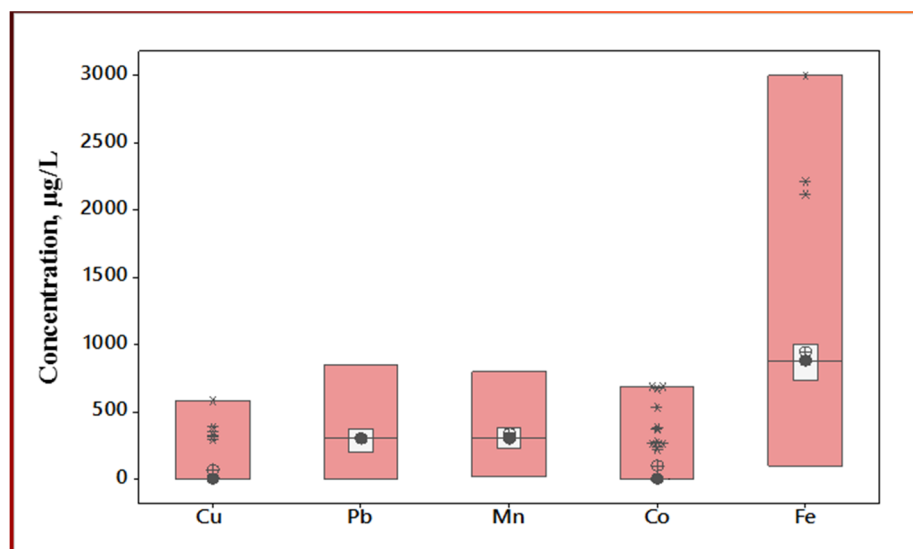


Figure 2. Box plot showing the measured trace elements distribution.

Inspection of the individual distributions in Figure 3 led to extracting the following remarks compared to the distribution of TC, Figure 3n, and *E. coli*, Figure 3o. Figure 3a showed an inverse temperature distribution to that of TC and *E. coli*, i.e., the northwest and southeast portions demonstrated higher water temperatures, are FB-free. This trend suggests an attenuation function of the temperature on FB with a more decisive effect on *E. coli*, i.e., *E. coli* is less tolerant to high temperatures. However, the temperature ranges encountered were not harsh to FB, which can withstand far higher values up to 120 °C [44,91,92], suggesting the existence of indirect effects of temperature. Power of hydrogen (pH, Figure 3b) showed no specific trend with the FB spatial distributions, which may be ascribed to that the pH values encountered in the study region are within the survivable range of FB, ranging from slightly acidic (6.8) to slightly alkaline (8.35). The effects of pH on die-off or FB's attenuation were reported to be significant at levels less than six and greater than nine [87,88], which is beyond those encountered in the study area.

DOC (Figure 3c) and DO (Figure 3d) exhibited antithesis distributions (i.e., the regions that show high levels of DOC and DO are the regions free of TC and *E. coli*), which seems logical as FB consume DOC and DO for survival and proliferation. Nevertheless, as clarified in the forthcoming sections, the story is different. Salinity or total dissolved solids (TDS) distribution, Figure 3e, was antagonistically distributed concerning FB, confirming the existence of a bacterial purification effect FB at elevated TDS levels. Moreover, this theme showed that TDS is a significant stressor on *E. coli* compared to TC, emphasizing the lesser tolerability (higher sensitivity) of *E. coli*. The higher TDS regions (dark brown colored ones) of SD correspond to the regions free of *E. coli* (yellow to light brown colored regions). The case for TC was similar to that for *E. coli* except with more spreading of the dark brownish regions of TC overlaying the light brown regions for TDS distribution, hinting at more ruggedness of TC compared to *E. coli* towards TDS. Effects of salinity on the mortality (purification) of different species and microbial communities gained significant scholars' interest, concluding that every community has its TDS range at which the microbes' cell

membranes can withstand the osmotic stresses. However, this range may be subjected to environmental adaptation to cope with higher TDS levels than originally [93–96]. According to the current findings, there was a threshold of salinity higher than it; no microbial communities were detected at 3500 mg/L and 6000 mg/L for *E.coli* and TC, respectively. Current findings agree and are corroborated by that of Akhavan et al.; they reported that with an increase in the ionic strength of the soil solution, the amount of bacterial purification was increased, which could effectively control groundwater contamination with saline water management since the least transition might occur [97]. Mamilov et al. reported that salinity presents large stresses on microorganisms since it decreases respiration, carbon dioxide levels, enzymatic activity, and microbial biomass [98]. Another path of FB retention is the adherence (adsorption) to the sand surface which is found to depend on many factors, including ionic strength (TDS), since with increasing TDS, the negative charge of subsurface deposits increases, leading to increased maintenance of bacteria due to the compression of the double layer that enhances equilibrium between the bacterial load and sediment [97].

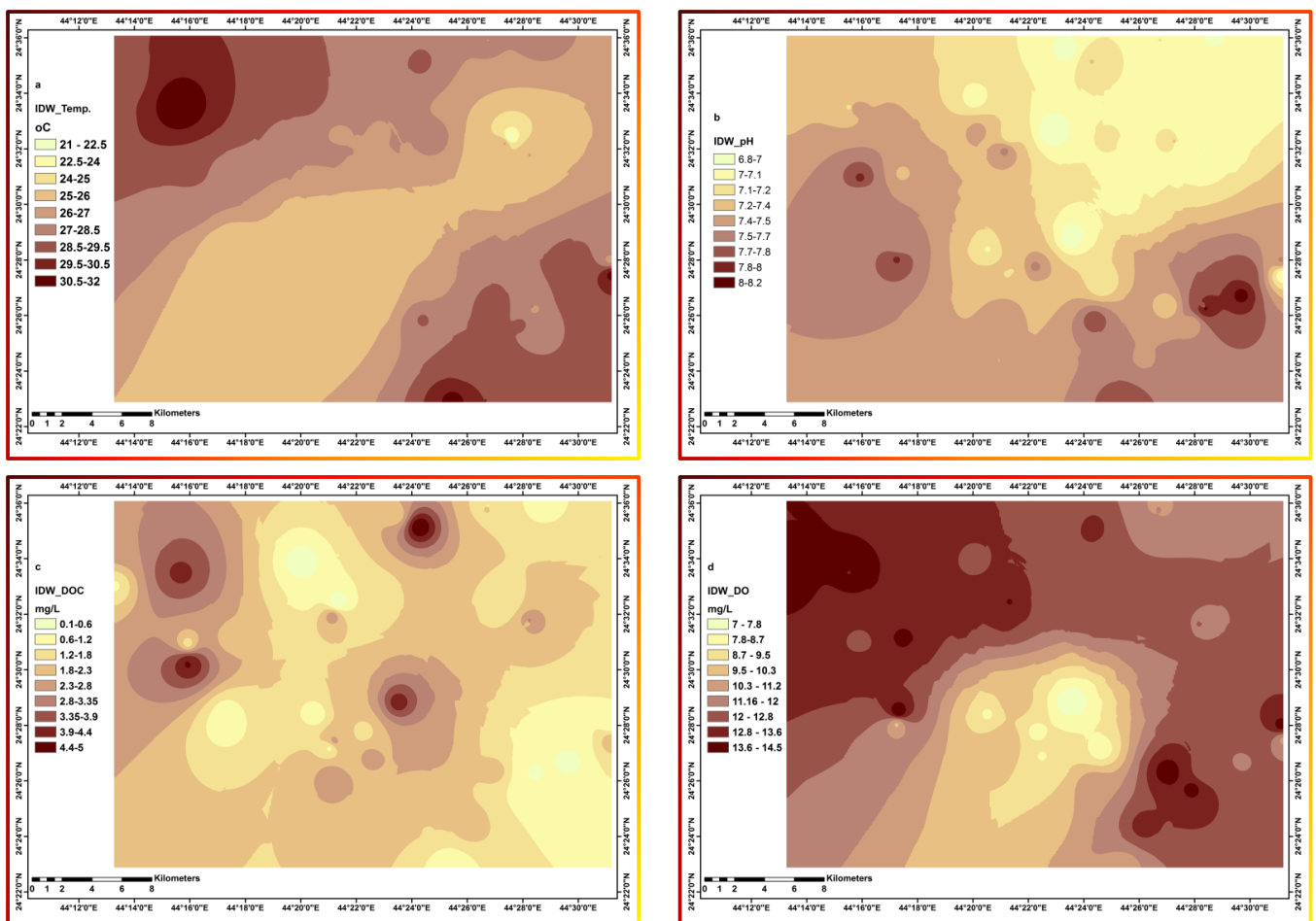


Figure 3. Cont.

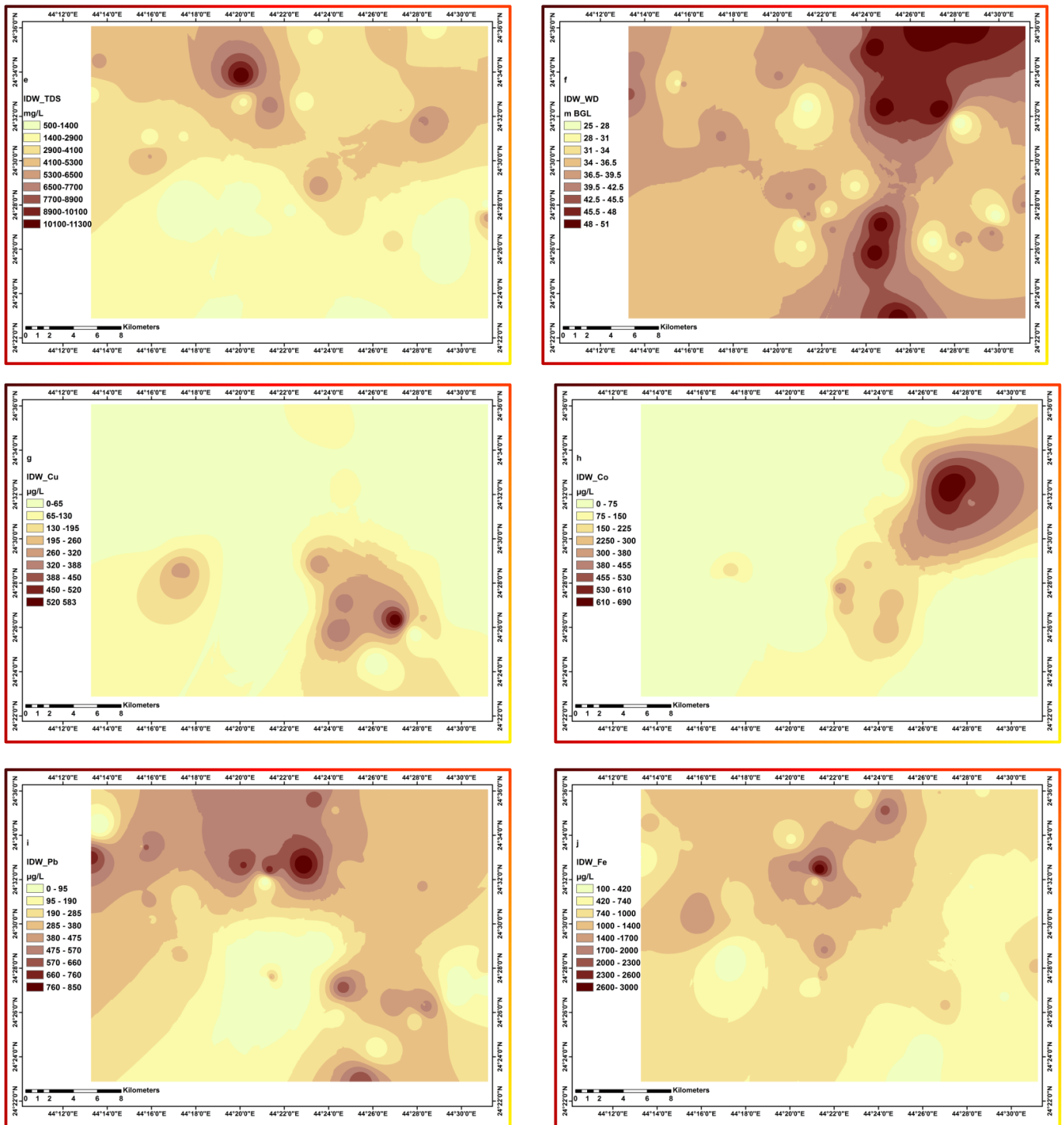
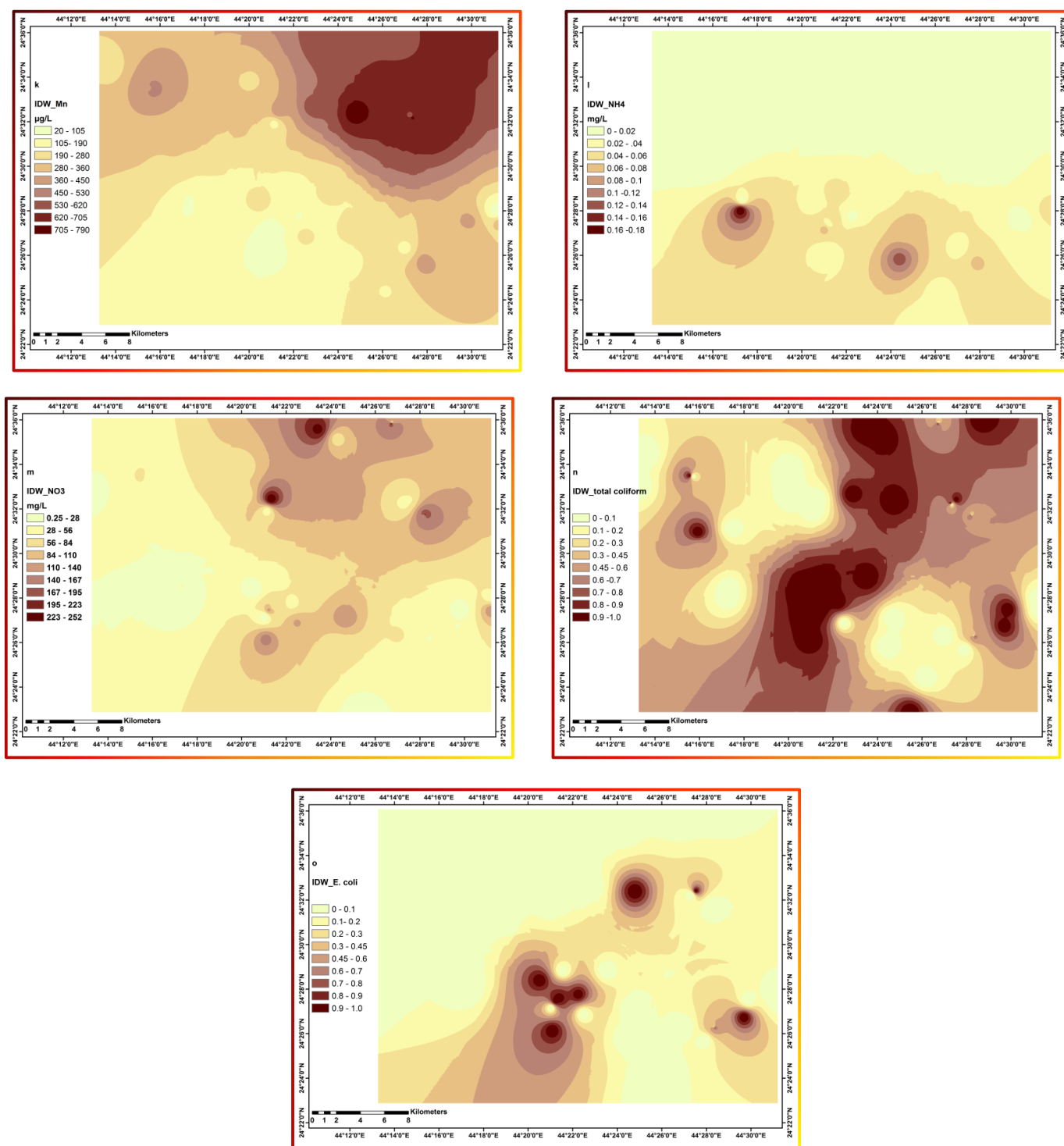


Figure 3. Cont.



**Figure 3.** Spatial distribution maps portraying spatial variability of the concerned parameters throughout the study area. The sub-graphs represent the SD distribution of individual parameters; (a): temperature; (b): pH; (c): dissolved organic carbon; (d): dissolved oxygen; (e): total dissolved solids; (f): well-depth; (g): Copper; (h): Cobalt; (i): Lead; (j): iron; (k): Manganese; (l): ammonium; (m): nitrate; (n): total coliform; and (o): *E. coli*.

Wells depths (Figure 3f) showed an inverse distribution to FB with few localized exceptions, per the findings of Dey et al. [97]. This distribution seems logical since the deeper wells implied longer travel times and contact with the hosting rocks exposing the FB to more frequent adsorption cycles imposing a less favorable environment and higher

stresses on the microbial communities' survivals. Again, a more prominent theme for *E. coli* than TC confirms the higher sensitivity of *E. coli*. Copper (Figure 3g) and Cobalt (Figure 3h) exhibited a worthy noting theme that the pockets of Cu and Co concentrations >195 and >150 µg/L, respectively, yielded negative test results for *E. coli* and TC demarcating a possible threshold of sterilization or hygienic effect of copper and cobalt. Lead (Figure 3i) and Iron (Figure 3j) concentrations showed similar effects as Cu and Co but with somewhat more spatial widespread and higher threshold values; Pb and Fe effective concentrations were >280 and 2000 µg/L, respectively. Manganese (Figure 3k) spreads over most of the study area, with the highest concentrations occurring in the northeastern part. Again, pockets of high Mn loads showed no *E. coli* and vice versa, with a far higher tolerance for TC, suggesting the presence of higher Mn hygienic effects on *E. coli* than TC. Ammonium (NH<sub>4</sub>) concentration distribution, Figure 3l, showed no rigid relationship with FB. Ammonium levels were consistently minimal throughout the study area, with many sampling points' contents below detection limits. However, there is a slight overlay distribution pattern in the southern part of the study area, suggesting their occurrence from a common source. Nitrate (Figure 3m) had a significant opposite relationship with TC and *E. coli*. Most locations positive for FB also have nitrate concentrations but lower concentrations than those in FB-free regions. This theme may be ascribed as that they have a common source, and FB, where present, consume nitrate for survival and proliferation.

Spatial distribution maps provided a good visualization tool enabling direct comparison of the spatial variabilities all over the study area for the concerned parameters. Inspection and comparing similarities and dissimilarities allowed valuable data mining, at least conceptually, that helps screen and select the effective parameters to go further within the subsequent analysis stages. The main limitation of the spatial distribution maps is their representation of one variable at a time without looking for the intercorrelations with other factors, whether bi- or multivariate correlations. The expected interactions, and embedded and remedied effects will be scrutinized from now on.

### 3.3. Interactions among the Interplaying Factors

This section looks further into the types and nature of interactions among the deemed significant parameters, as identified from the spatial distribution maps in the previous section. The scatter box plot matrix collectively addresses such interactions, Figure 4. The scatter box plot matrix explores the interrelationships among the individual parameters, explicitly showing the changes point by point in contrast to the implicit averaging employed in spatial distribution maps. This approach has the pros of clarifying the extremes and the exact interactions in the studied region between every two parameters otherwise masked in the smoothed interpolated themes. Nevertheless, it has the shortcoming of the disability to mark the interaction spatially. Hence, integrating the information extracted from both approaches helps constrain each approach's conclusions, reducing the implied uncertainty budgets. As Figure 4 shows, the TDS has a prominent effect on *E. coli*, i.e., above ≈3500 mg/L, there no *E. coli* detected. While TC tolerates approximately double, i.e., ≈6500 mg/L, which is in close agreement with the thresholds extracted from the SD methods. On the contrary, temperature showed that TC spans over the whole temperature range, which disagrees with SD findings. *E. coli* were not detected above 29 °C, exhibiting good agreement with the SD findings. The pH exhibited a remarkable effect as most samples that tested positive for FB were at pH levels >7.8. Such behavior may be explained as at pHs higher than 7.8, the concentration of heavy metals goes down, especially for Cu, Co, and Fe. These effects corroborate the SD findings that heavy metals concentrations are significant for the survival of microbial communities. The WD, NO<sub>3</sub>, and DO parameters showed no effects on TC, i.e., TC are present all over the whole span of those parameters. *E. coli* exhibited the exact change as TC except for DO, DOC, and NO<sub>3</sub><sup>-</sup> which showed no *E. coli* detected at higher levels of the parameters. Such findings may be due to other factors rather than parameters-specific effects since *E. coli* tested positive for only a limited number of samples—20%.

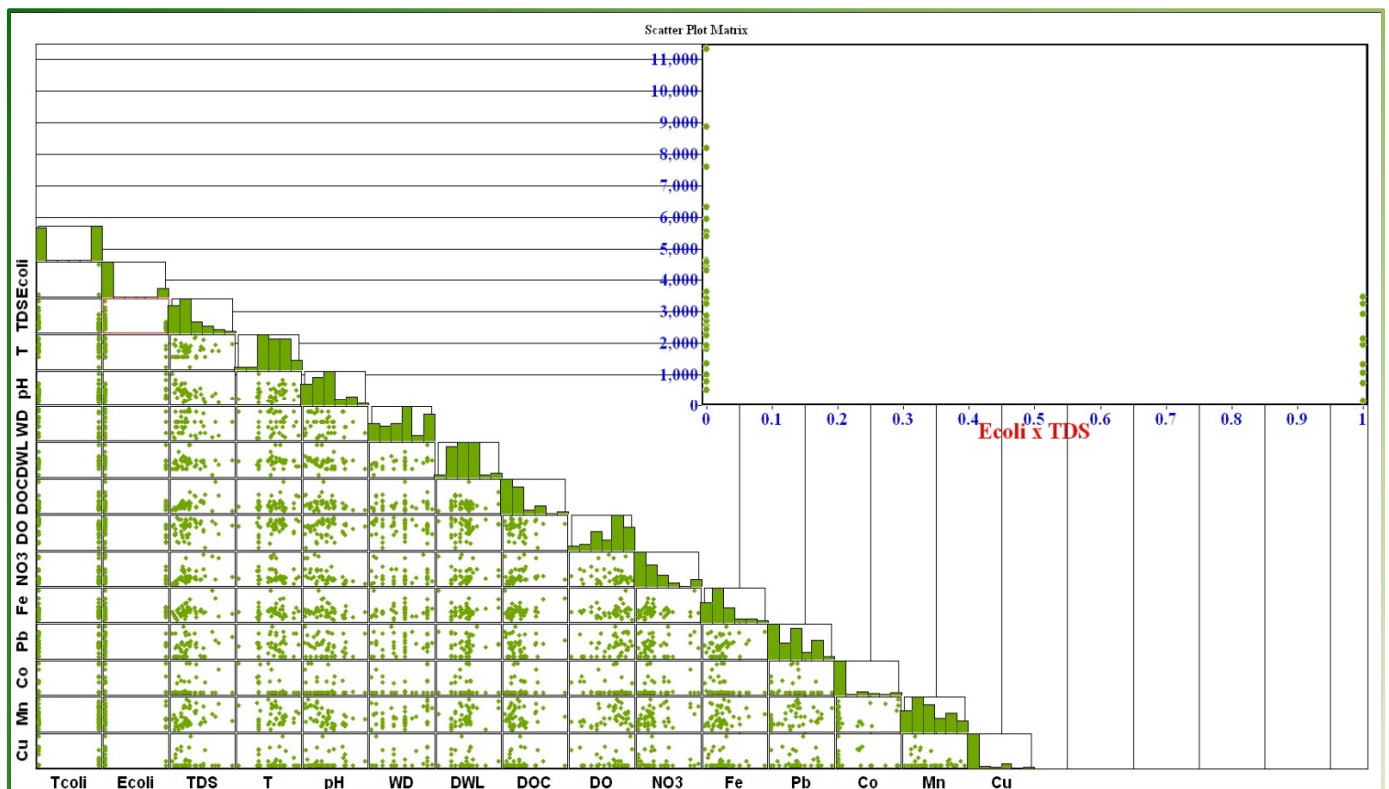


Figure 4. Scatter box plot matrix of the interplaying factors.

The parameters Mn, Co, and Pb manifested no effects on TC and *E. coli*, which opposed the SD conclusions. These discrepancies constrain the SD conclusions suggesting that the confounding patterns were due to variables other than those related to the measured parameters. On the other hand, Fe concentrations exhibited an antagonistic relationship at higher levels, 2000 and 1200  $\mu\text{g}/\text{L}$  for TC and *E. coli*, respectively, which agrees well with SD results. Similarly, the Cu concentration exposed an antagonistic effect at 300 and 100  $\mu\text{g}/\text{L}$  thresholds for TC and *E. coli*, respectively, agreeing with SD findings. Overall, the scatter box plot matrix help constrain the SD findings providing multiple lines of evidence. This approach help screen the significant variables as the factors that showed agreement in both approaches might be identified as the most effective ones and vice versa. A step forward may be carried out by analyzing the cumulative and synergistic effects of parameters expected to play a profound role in FB elimination or presence. Further investigation into such deemed corroborated or contradicted effects by the significant factors delineated from the above sections follows.

### 3.4. Synergistic Effects

In the preceding section, the binary correlations, i.e., the effect of one variable at a time on the response, the FB, were investigated. This section investigates the synergistic effects of two variables at a time on FB, deeming that it will provide good insights into the correlations under consideration. Bubble diagrams and the 3D surface plots are the chosen type with each variable per axis, and the radii of the bubbles represent the absence or presence of the response factor, FB. In addition, TC and *E. coli* were superimposed on the same plot with different colors. This way, the cooccurrence or absence of the FB could be visualized as a function of the axes variables.

TDS and temperature showed a significant effect on coliform, especially *E. coli*. The two factors' coexistence effects are portrayed in the bubble plot, Figure 5. TDS has a profound effect, and FB cannot withstand higher TDS levels with a higher tolerance for TC than *E. coli*, agreeing with the SD and the scatter box plot matrix findings. As Figure 5

reveals, there appears to be a declining trend, as in the case of high TDS, the temperatures at which samples tested positive were reduced.

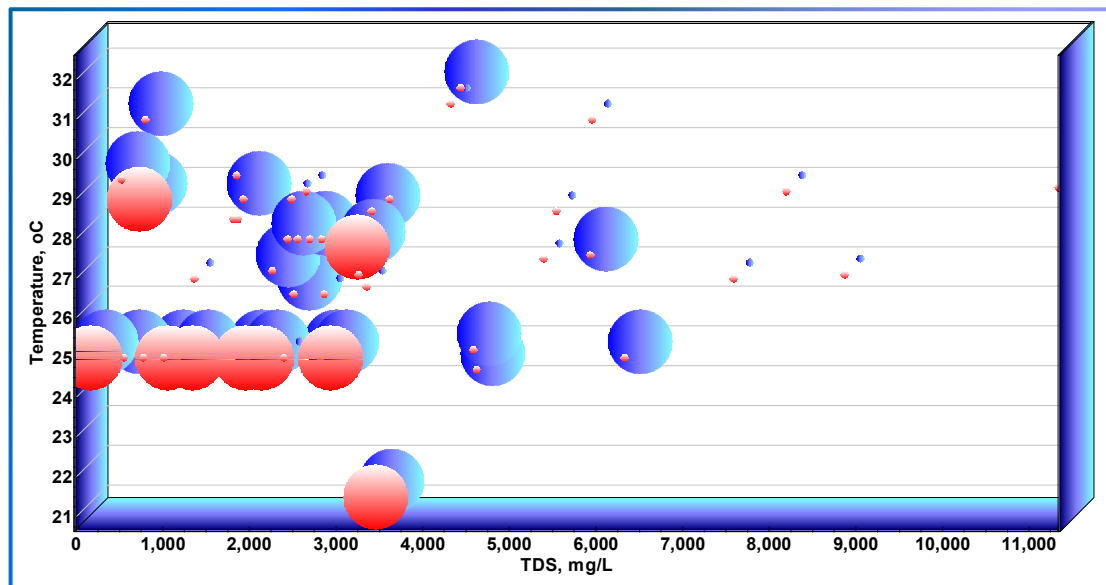


**Figure 5.** Bubble plot of the TDS and Temperature combined interaction on TC (blue) and *E. coli* (red).

TDS and pH portrayed in Figure 6 showed that coliforms span all over the range at the low TDS levels. With TDS going up, *E. coli* was not detected at pH > 7.8. The prominent effect may be due to TDS only as the large bubbles span all over the whole pH range. However, the pH may influence indirectly via its inverse relationship with TDS. This theme constrains the scatter box plot matrix inferences. TDS and Cu concentration manifested a significant influence on coliform, especially *E. coli*, as evident in Figure 7. The effect of Cu is most prominent, and no sample tested positive for *E. coli* at a Cu concentration above 150 µg/L, which agrees well with the preceding findings of SD and box plot matrix. Worth noting is that although copper occurred only in samples of low TDS, as seen in the left fringe of the plot, the exhibited effective hygienic influence emphasizes no synergism between TDS and Cu. Moreover, the effect of Cu is expressed clearly with a much higher tolerance towards Fe, as shown in Figure 8, which opposed the preceding inferences concerning iron effects, as TC and *E. coli* bubbles span most of the entire range of Fe concentrations. Again, this trend constrains the preceding SD and box plot matrix findings.

Well-depth was expected to be an influencing factor from SD and box plot matrix. Nevertheless, Figure 9 shows that this is not the case with the FB detected in all wells, whatever their depths are, as evident from their span all over the whole range, with the Cu effects being the most prominent. NO<sub>3</sub><sup>-</sup> correlation inferred from SD and box plot matrix was inversely related with TC and *E. coli*, with the most prominent for *E. coli*. The combined effects of NO<sub>3</sub><sup>-</sup> and Fe concentrations shown in Figure 10 agree with the inference concerning *E. coli* but constrain such a conclusion for the TC case. Furthermore, a neutral relationship between FB and Fe is apparent, along with an inverse relationship between NO<sub>3</sub><sup>-</sup> and Fe such that NO<sub>3</sub><sup>-</sup> concentrations are lower at elevated Fe levels. Worth noting is the presence and absence of FB in all ranges of Fe and NO<sub>3</sub><sup>-</sup>, emphasizing the existence of no relationship constraining, contradicting the SD and box plot matrix findings again. A similar neutral relationship was observed for Pb and Fe on FB, Figure 11, confirming that coliform bacteria are tolerant to Fe and Pb concentrations. DOC and DO exhibited opposite SD with FB corroborated by the box plot findings. Figure 12 shows the same but significantly loosened relationship as there were specific discriminated regions except for *E. coli*, which is absent at high DO and DOC concentrations.

Moreover, the 3D surface plot represents good visualization of the covariance of three factors at a time on the response, which helps figure out more constrained evidence for the main stressor on the response parameter, FB. Figure 13 exhibits the correlation of  $\text{NO}_3$ , and Cu concentration on TC, left, and *E. coli* (right). As evident, *E. coli* tested positive at lower concentrations of nitrate and copper, with the effects of copper much more prominent. A somewhat different pattern is noted for TC, expressing its higher nitrate tolerance spanning the whole range of nitrate concentrations except the extremely high values, the most right downward tail. A similar trend is evident in Figure 14 for the co-effects of Cu and Fe.

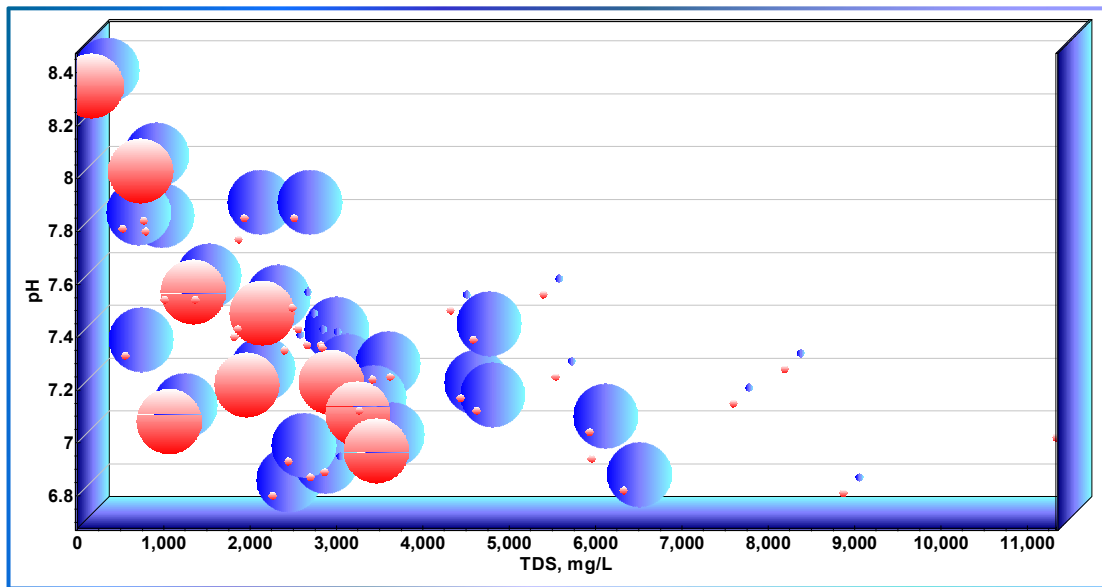


Figure 6. Bubble plot of the TDS and pH combined interaction on TC (blue) and *E. coli* (red).

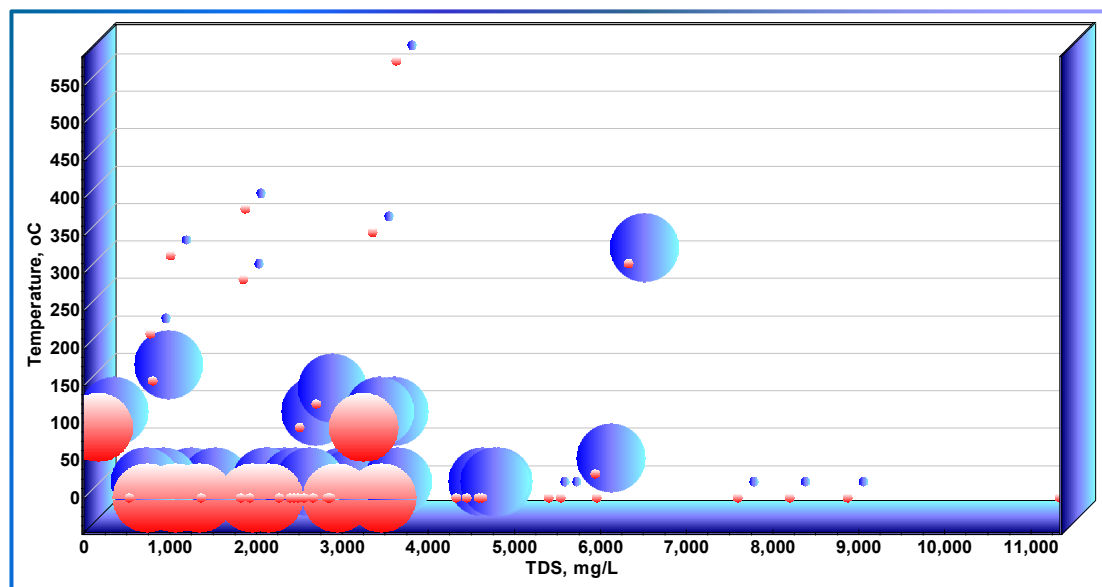


Figure 7. Bubble plot of the TDS and Cu concentration combined interaction on TC (blue) and *E. coli* (red).

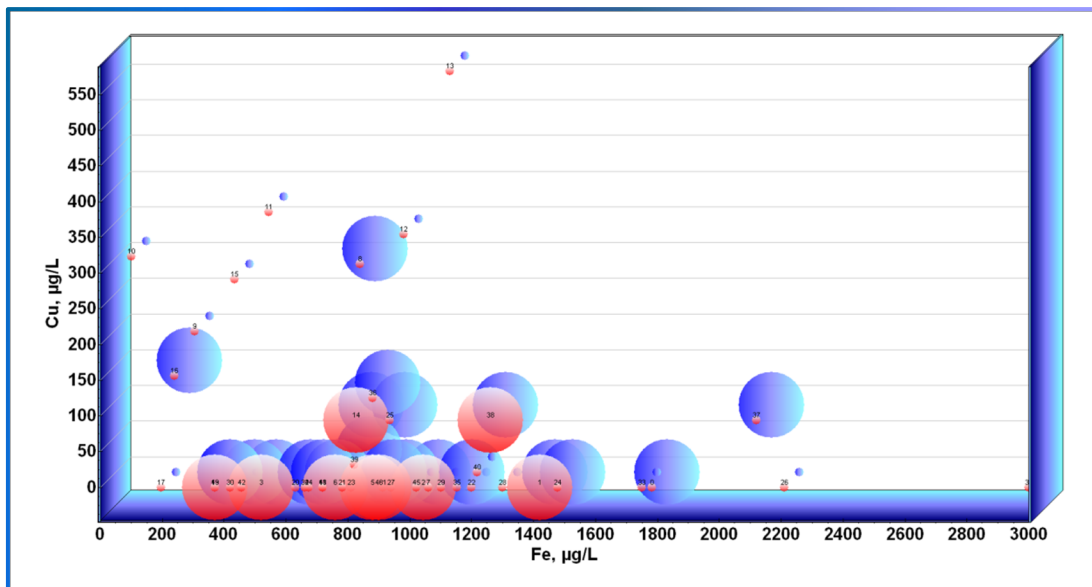


Figure 8. Bubble plot of the Fe and Cu concentrations combined interaction on TC (blue) and *E. coli* (red).

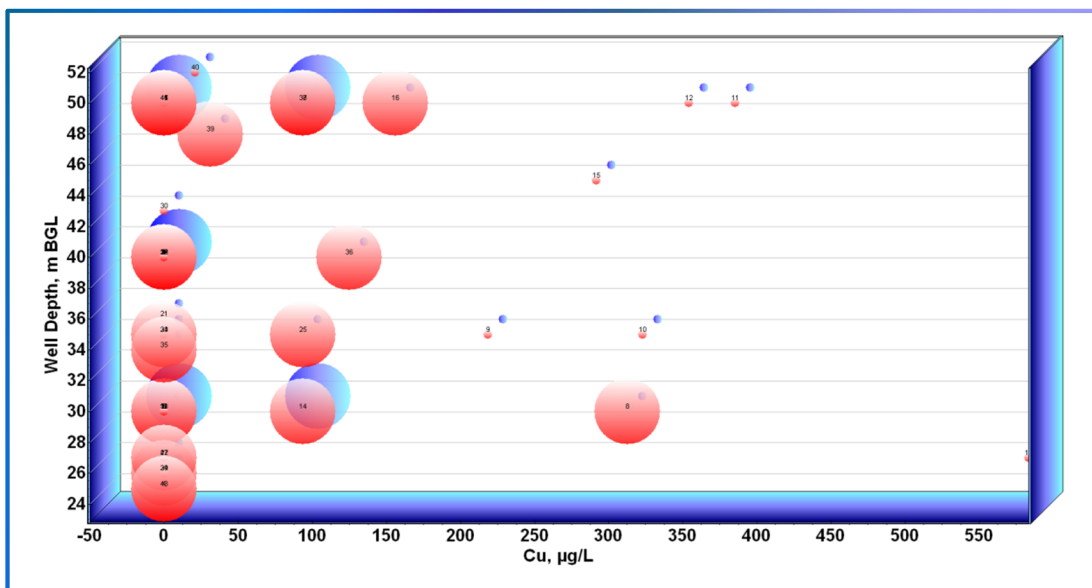


Figure 9. Bubble plot of the well depth and Cu concentrations combined interaction on TC (blue) and *E. coli* (red).

Many different combinations were plotted (not shown, avoiding lengthy), which mostly yielded more or less similar trends concluded above. The identified themes of differences between *E. coli* and TC may be ascribed partially to the difference in the number of tested positive samples. The smaller number of samples positive for *E. coli*, accompanied by its limited spatial distribution, may lead to such discrepancies.

### 3.5. Spearman Rho Correlation Analysis

Statistical testing of correlation measures how two variables change together, describing the relationship’s strength and direction. It has found significant room for application and has been routinely applied in recent years. Spearman’s rho measures the monotonic relationship between two continuous or ordinal variables. Although TC and *E. coli* are ordinal variables, correlation testing is claimed to yield erroneous results due to numerical nonconformity between the interplaying factors, especially for factors with a wide span

of numbers like trace elements and TDS. Moreover, Spearman’s correlation coefficients measure only monotonic (linear) relationships, and a meaningful relationship can exist even if the correlation coefficients are zero, making examining a scatter box plot determining the relationship more beneficial. Hence, the current demonstration provides statistical testing to compare with the findings of the visualization-based ones. Table 2 presents the abbreviated list of coefficients showing only those related to *E. coli* and TC. The correlations rank as strong, medium, and low when the coefficients are >0.7, 0.5–0.7, and <0.5, with positive factors indicating a direct relation and vice versa. The test requires that the *p*-value be <0.05 to be significant at a 95% confidence level. Accordingly, if present, all correlations fall within the low rank.

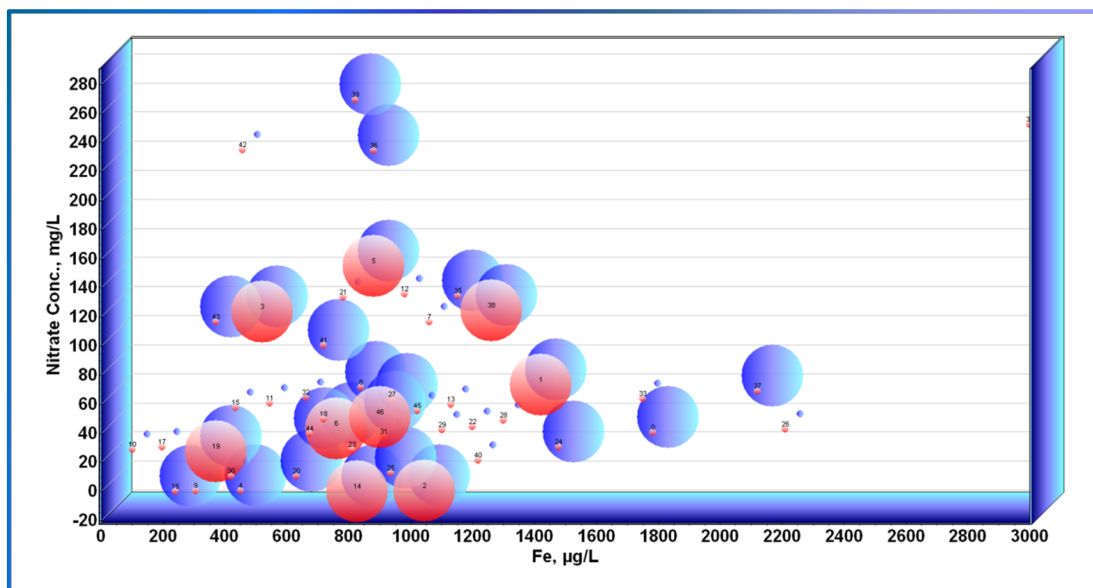


Figure 10. Bubble plot of the Nitrate and Fe concentrations combined interaction on TC (blue) and *E. coli* (red).

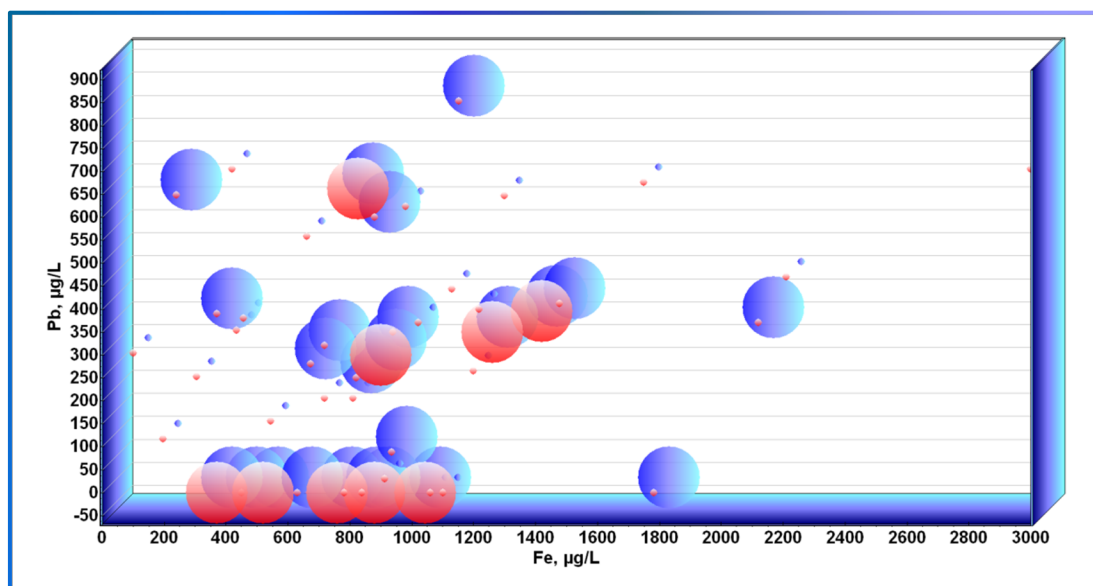


Figure 11. Bubble plot of the Pb and Fe concentrations combined interaction on TC (blue) and *E. coli* (red).

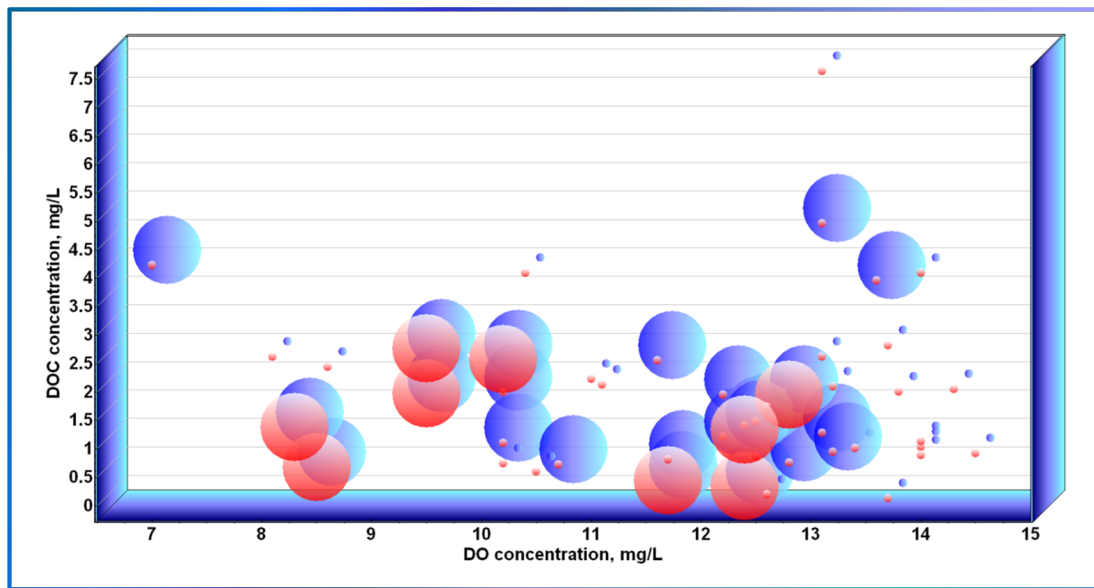


Figure 12. Bubble plot of the Pb and Fe concentrations combined interaction on TC (blue) and *E. coli* (red).

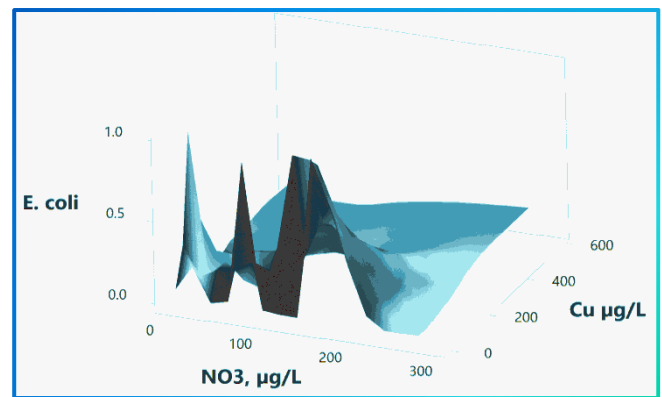
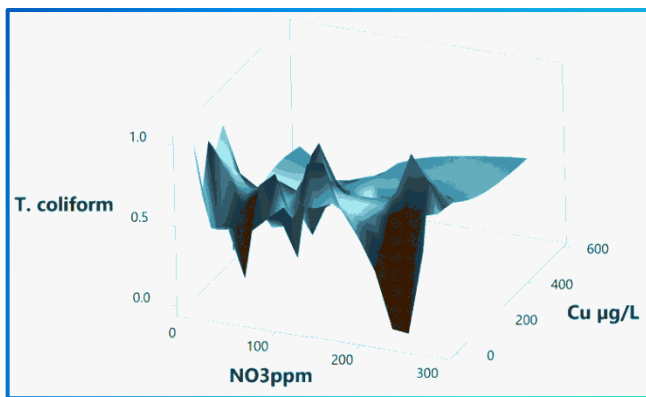


Figure 13. 3D surface plot of the combined interactions of Cu and nitrate concentrations on TC (left) and *E. coli* (right).

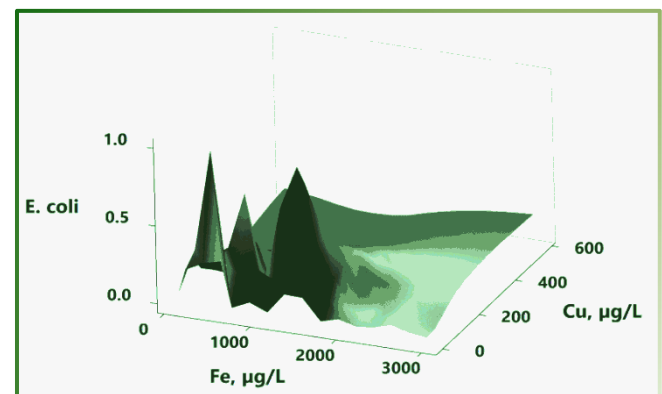
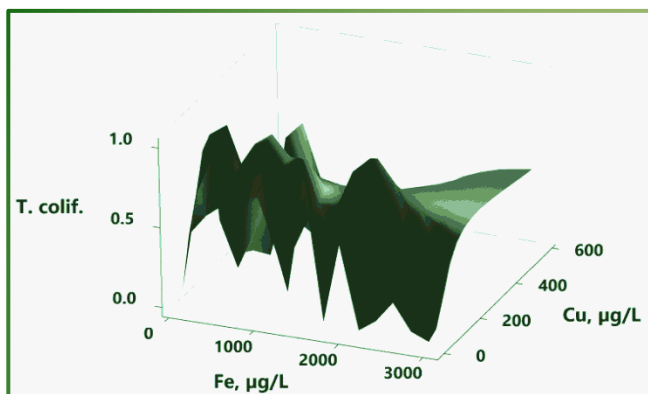


Figure 14. 3D surface plot of the combined interactions of Cu and Fe concentrations on TC (left) and *E. coli* (right).

**Table 2.** Output matrix of the 1:1 Spearman's rho correlation test.

Parameter	Total Coliform	<i>E. coli</i>	Parameter	Total Coliform	<i>E. coli</i>	Parameter	Total Coliform	<i>E. coli</i>
<i>E. coli</i>	0.476		Appearance	0.082	0.034	Cu µg/L	−0.038	−0.133
<i>p</i> -Value	0.001		<i>p</i> -Value	0.586	0.823	<i>p</i> -Value	0.800	0.374
Temp	−0.298	−0.408	Odor	0.144	0.303	Pb µg/L	−0.193	−0.233
<i>p</i> -Value	0.042	0.004	<i>p</i> -Value	0.333	0.038	<i>p</i> -Value	0.194	0.115
pH	−0.044	0.072	WD, m BGL	−0.062	0.039	Mn µg/L	0.107	−0.146
<i>p</i> -Value	0.769	0.632	<i>p</i> -Value	0.677	0.797	<i>p</i> -Value	0.475	0.328
TDS, mg/L	−0.235	−0.291	Disch., m <sup>3</sup> /d	0.142	−0.059	Co µg/L	−0.014	0.136
<i>p</i> -Value	0.111	0.047	<i>p</i> -Value	0.343	0.692	<i>p</i> -Value	0.928	0.364
DO, mg/L	−0.394	−0.369	NH <sub>4</sub> , mg/L	−0.128	0.136	Fe µg/L	−0.014	0.136
<i>p</i> -Value	0.006	0.011	<i>p</i> -Value	0.390	0.362	<i>p</i> -Value	0.928	0.364
DOC, mg/L	−0.066	−0.114	NO <sub>3</sub> , mg/L	0.006	−0.008			
<i>p</i> -Value	0.660	0.447	<i>p</i> -Value	0.967	0.958			

Inspection of the factors yielded an agreement with the SD for *E. coli* and TC as they have a common source, as expected in the southern part of the study area. The correlation factor states the presence of a low correlation between both factors without marking where such correlation prevails spatially. This cooccurrence in the southern part only could be explained by the TDS that increases from south to north. Temperature yields a low inverse correlation with *E. coli* higher than that for TC. Again, those inverse correlation factors suggest an attenuation effect of temperature that is not evident through the preceding sections except for a small range free of *E. coli* at temperatures >30 °C. TDS showed no significant Spearman's rho correlation, which contradicts the findings of SD, binary, and tertiary interactions for T. coliform. However, TDS exhibited a low inverse significance Spearman's correlation in the case of *E. coli*, supporting the findings of SD, binary, and tertiary interactions. Cu concentration demonstrated a major role in the coliform distribution in the preceding sections, especially of *E. coli*. However, it yields no Spearman's rho correlation. The other studied variables yielded no Spearman's rho correlations that explicitly contradicted the identified themes. Those discrepancies may be because the test initially seeks linear relationships. The data represented here with presence/absence test results for the concerned parameters have a cutoff relationship (threshold) rather than a linear one which might not be the case if the quantitative assessment for the colonies is the adopted analysis.

Overall, the statistical correlation analysis yields limited and sometimes erroneous information and should be dealt with with great care. However, integrating all suitable data analysis methods may enhance the confidence of the inferences, constrain and contrast the findings, and reduce the associated uncertainty budgets.

#### 4. Conclusions

Fecal bacteria in groundwater wells have been identified for decades, with recent studies conducted to discriminate and quantify how hydrogeological and non-hydrogeological parameters correlate with their occurrence. The current work mainly presents some methodological aspects to understanding the effects of physicochemical and hydrogeological factors on FB behavior that may contribute to developing better procedures to protect water quality and improve human health outcomes. In this study, the influential factors affecting fecal bacteria in the groundwater aquifer of a hyperarid area facing recent prolonged drought periods, Ad-Dawadmi, KSA, have been identified. The authors adopted the visualizations-based methodologies in a graded approach to conceptually mine the interplaying correlations among different types of hydrological and physicochemical factors with the presence/absence of TC and *E. coli* as the response parameters. The main inferences can be summarized as follows:

- a. *E. coli* has higher sensitivity and less tolerability than TC towards the adversely influencing factors.

- b. Nitrate, DOC, and DO showed to be inversely distributed concerning the occurrence of fecal bacteria. Their quasi-random distribution may counteract the validity of their usage as coliforms surrogates.
- c. TDS exhibited a purification effect at  $\approx 3500$  mg/L and  $\approx 6000$  mg/L for *E. coli* and TC, respectively.
- d. The copper concentration effect was similar to TDS at 150 and 300  $\mu\text{g/L}$  thresholds for *E. coli* and TC, respectively.
- e. The occurrence of FB in deep boreholes (30–52 m) with approximately no precipitation during the last five years challenges the sole water source that significantly threatens the region's public health.
- f. Integrating various types of analyses was found to be powerful, as it helped constrain and provide multiple lines of evidence for the concluded remarks.
- g. A statistical Spearman's rho correlation analysis yielded no consistent results with other methods due to the absence of the linear relationship that the test seeks.

Discerning the influential water quality factors concerning fecal bacteria and their effectiveness could provide prior knowledge for accurate management of human activities and help screen, prioritize, and select the quality monitoring parameters. Finally, the followed approach and methodology proved to figure out the otherwise hidden correlations adequately, along with the advantages of having ease of construction and conduct, being directly readable and interpretable visualizations, being free of confusing or hidden discrepancies, and providing spatially-related inferences when integrated.

**Author Contributions:** Conceptualization, H.E.G., A.A.A. and F.A.G.; methodology, H.E.G., M.C., A.A.A. and F.A.G.; software, H.E.G. and F.A.G.; validation, A.A.A., A.H.A. and H.E.G.; formal analysis, H.E.G. and M.C.; investigation, H.E.G., M.C. and F.A.G.; resources, A.A.A. and H.E.G.; data curation, A.A.A. and F.A.G.; writing—original draft preparation, H.E.G. and F.A.G.; writing—review and editing, A.A.A., F.A.G., M.C. and A.H.A.; visualization, H.E.G. and F.A.G.; supervision, H.E.G.; project administration, H.E.G.; funding acquisition, H.E.G. All authors have read and agreed to the published version of the manuscript.

**Funding:** The authors extend their appreciation to the Deputyship for Research & Innovation, Ministry of Education in Saudi Arabia, for funding this research work through the project number (IFP2021-062).

**Institutional Review Board Statement:** Not applicable.

**Informed Consent Statement:** Not applicable.

**Data Availability Statement:** Not applicable.

**Conflicts of Interest:** The authors declare no conflict of interest. The funders had no role in the design of the study; in the collection, analyses, or interpretation of data; in the writing of the manuscript, or in the decision to publish the results.

## References

1. Jha, M.K.; Shekhar, A.; Jenifer, M.A. Assessing Groundwater Quality for Drinking Water Supply Using Hybrid Fuzzy-GIS-Based Water Quality Index. *Water Res.* **2020**, *179*, 115867. [[CrossRef](#)] [[PubMed](#)]
2. Qu, S.; Shi, Z.; Liang, X.; Wang, G.; Han, J. Multiple Factors Control Groundwater Chemistry and Quality of Multi-Layer Groundwater System in Northwest China Coalfield—Using Self-Organizing Maps (SOM). *J. Geochem. Explor.* **2021**, *227*, 106795. [[CrossRef](#)]
3. Dehnavi, A.; Sarikhani, R.; Nagaraju, D. Hydro Geochemical and Rock Water Interaction Studies in East of Kurdistan, NW of Iran. *Int. J. Environ. Sci. Res.* **2011**, *1*, 16–22.
4. Subramani, T.; Rajmohan, N.; Elango, L. Groundwater Geochemistry and Identification of Hydrogeochemical Processes in a Hard Rock Region, Southern India. *Environ. Monit. Assess.* **2010**, *162*, 123–137. [[CrossRef](#)] [[PubMed](#)]
5. Kumar, P.; Mahajan, A.K.; Kumar, A. Groundwater Geochemical Facie: Implications of Rock-Water Interaction at the Chamba City (HP), Northwest Himalaya, India. *Environ. Sci. Pollut. Res.* **2019**, *27*, 9012–9026. [[CrossRef](#)]
6. Su, Y.-H.; Feng, Q.; Zhu, G.-F.; Si, J.-H.; Zhang, Y.-W. Identification and Evolution of Groundwater Chemistry in the Ejin Sub-Basin of the Heihe River, Northwest China. *Pedosphere* **2007**, *17*, 331–342. [[CrossRef](#)]

7. Lotfi, S.; Chakit, M.; Najy, M.; Talbi, F.Z.; Benchahid, A.; El Kharrim, K.; Belghyti, D. Assessment of Microbiological Quality of Groundwater in the Saïs Plain (Morocco). *Egypt. J. Aquat. Biol. Fish.* **2020**, *24*, 509–524. [[CrossRef](#)]
8. Xin, J.; Wang, Y.; Shen, Z.; Liu, Y.; Wang, H.; Zheng, X. Critical Review of Measures and Decision Support Tools for Groundwater Nitrate Management: A Surface-to-Groundwater Profile Perspective. *J. Hydrol.* **2021**, *598*, 126386. [[CrossRef](#)]
9. Chen, H.; Teng, Y.; Lu, S.; Wang, Y.; Wu, J.; Wang, J. Source Apportionment and Health Risk Assessment of Trace Metals in Surface Soils of Beijing Metropolitan, China. *Chemosphere* **2016**, *144*, 1002–1011. [[CrossRef](#)]
10. US EPA Seminar Publication. *Groundwater Contamination; Wellhead Protection: A Guide for Small Communities*. Chapter 3. EPA/625/R-93/002. Available online: <chrome-extension://efaidnbmnndpckcjpcglclefindmkaj/https://www.epa.gov/sites/default/files/2015-08/documents/mgwc-gwc1.pdf> (accessed on 9 October 2022).
11. Griesel, M.; Jagals, P. Faecal Indicator Organisms in the Renoster Spruit System of the Modder-Riet River Catchment and Implications for Human Users of the Water. *Water SA* **2002**, *28*, 227–234. [[CrossRef](#)]
12. Aram, S.A.; Saalidong, B.M.; Lartey, P.O. Comparative Assessment of the Relationship between Coliform Bacteria and Water Geochemistry in Surface and Ground Water Systems. *PLoS ONE* **2021**, *16*, e0257715. [[CrossRef](#)] [[PubMed](#)]
13. Ramírez-Castillo, F.Y.; Loera-Muro, A.; Jacques, M.; Garneau, P.; Avelar-González, F.J.; Harel, J.; Guerrero-Barrera, A.L. Waterborne Pathogens: Detection Methods and Challenges. *Pathogens* **2015**, *4*, 307–334. [[CrossRef](#)] [[PubMed](#)]
14. Dzwaïro, B.; Hoko, Z.; Love, D.; Guzha, E. Assessment of the Impacts of Pit Latrines on Groundwater Quality in Rural Areas: A Case Study from Marondera District, Zimbabwe. *Phys. Chem.* **2006**, *31*, 779–788. [[CrossRef](#)]
15. Cabral, J.P.S.; Center Water Microbiology. Bacterial Pathogens and Water. *Int. J. Environ. Res. Public Health* **2010**, *7*, 3657–3703. [[CrossRef](#)]
16. WHO. *Guidelines for Drinking-Water Quality*, 4th ed.; WHO: Geneva, Switzerland, 2017.
17. Albaggar, A. Saudi Journal of Biological Sciences Investigation of Some Physical, Chemical, and Bacteriological Parameters of Water Quality in Some Dams in Albaha Region, Saudi Arabia. *Saudi J. Biol. Sci.* **2021**, *28*, 4605–4612. [[CrossRef](#)]
18. Seo, M.; Lee, H.; Kim, Y. Relationship between Coliform Bacteria and Water Quality Factors at Weir Stations in the Nakdong River, South Korea. *Water* **2019**, *11*, 1171. [[CrossRef](#)]
19. Bryan, S.W.S. Coliform Bacteria. Available online: <https://extension.psu.edu/coliform-bacteria> (accessed on 28 October 2022).
20. Neill, M. Microbiological Indices for Total Coliform and *E. Coli* Bacteria in Estuarine Waters. *Mar. Pollut. Bull.* **2004**, *49*, 752–760. [[CrossRef](#)]
21. Armah, F.A. Relationship Between Coliform Bacteria and Water Chemistry in Groundwater Within Gold Mining Environments in Ghana. *Water Qual. Expo. Health* **2014**, *5*, 183–195. [[CrossRef](#)]
22. GSO 149/2014; Unbottled Drinking Water. GCC Standardization Organization (GSO): Riyadh, Saudi Arabia, 2014.
23. Herschy, R.W. Water Quality for Drinking: WHO Guidelines. In *Encyclopedia of Lakes and Reservoirs*; Encyclopedia of Earth Sciences Series; Bengtsson, L., Herschy, R.W., Fairbridge, R.W., Eds.; Springer: Dordrecht, The Netherlands, 2012. [[CrossRef](#)]
24. Huang, X.-Y.; Zhang, D.; Zhao, Z.-Q.; Liu, Y.-T.; Meng, H.-Q.; Zou, S.; Ma, B.-J.; Feng, Q.-Y. Determining Hydrogeological and Anthropogenic Controls on N Pollution in Groundwater beneath Piedmont Alluvial Fans Using Multi-Isotope Data. *J. Geochem. Explor.* **2021**, *229*, 106844. [[CrossRef](#)]
25. Macler, B.A.; Merkle, J.C. Current Knowledge on Groundwater Microbial Pathogens and Their Control. *Hydrogeol. J.* **2000**, *8*, 29–40. [[CrossRef](#)]
26. Poulin, C.; Peletz, R.; Ercumen, A.; Pickering, A.J.; Marshall, K.; Boehm, A.B.; Khush, R.; Delaire, C. What Environmental Factors in FI Uence the Concentration of Fecal Indicator Bacteria in Groundwater? Insights from Explanatory Modeling in Uganda and Bangladesh. *Environ. Sci. Technol.* **2020**, *54*, 13566–13578. [[CrossRef](#)]
27. Subba Rao, N.; Marghade, D.; Dinakar, A.; Chandana, I.; Sunitha, B.; Ravindra, B.; Balaji, T. Geochemical Characteristics and Controlling Factors of Chemical Composition of Groundwater in a Part of Guntur District, Andhra Pradesh, India. *Environ. Earth Sci.* **2017**, *76*, 747. [[CrossRef](#)]
28. Barba, C.; Folch, A.; Sanchez-vila, X.; Martínez-alonso, M.; Gaju, N. Are Dominant Microbial Sub-Surface Communities Affected by Water Quality and Soil Characteristics? *J. Environ. Manag.* **2019**, *237*, 332–343. [[CrossRef](#)] [[PubMed](#)]
29. Tropea, E.; Hynds, P.; Mcdermott, K.; Brown, R.S.; Majury, A. Environmental Adaptation of *E. Coli* within Private Groundwater Sources in Southeastern Ontario: Implications for Groundwater Quality Monitoring and Human Health. *Environ. Pollut.* **2021**, *285*, 117263. [[CrossRef](#)]
30. Abed, S.M.; Alaraji, K.H.Y.; Essa, R.H. Assessment of the Biological and Physiochemical Properties of Groundwater in Al-Muthanna Province, Iraq. *Eur. Asian J. Biosci.* **2020**, *5432*, 5425–5432.
31. Murray, R.T.; Rosenberg Goldstein, R.E.; Maring, E.F.; Pee, D.G.; Aspinwall, K.; Wilson, S.M.; Sapkota, A.R. Prevalence of Microbiological and Chemical Contaminants in Private Drinking Water Wells in Maryland, Usa. *Int. J. Environ. Res. Public Health* **2018**, *15*, 1686. [[CrossRef](#)]
32. Thériault, A.; Duchesne, S. Quantifying the Fecal Coliform Loads in Urban Watersheds by Hydrologic/Hydraulic Modeling: Case Study of the Beauport River Watershed in Quebec. *Water* **2015**, *7*, 615–633. [[CrossRef](#)]
33. Gorems, W.; Sisay, A. Fecal Coliform Bacteria Extent and Distribution Assessment in Lake Hawassa Fecal Coliform Bacteria Extent and Distribution Assessment in Lake Hawassa Watershed. *J. Med. Physiol. Biophys.* **2018**, *50*, 25–33.
34. Akpataku, K.V.; Gnazou, M.D.T.; Yawo, T.; Nomesi, A. Physicochemical and Microbiological Quality of Shallow Groundwater in Lomé, Togo. *J. Geosci. Environ. Prot.* **2020**, *8*, 162–179. [[CrossRef](#)]

35. Howard, G.; Pedley, S.; Barrett, M.; Nalubega, M.; Johal, K. Risk Factors Contributing to Microbiological Contamination of Shallow Groundwater in Kampala, Uganda. *Water Res.* **2003**, *37*, 3421–3429. [[CrossRef](#)]
36. Dwyer, J.O.; Chique, C.; Weatherill, J.; Hynds, P. Impact of the 2018 European Drought on Microbial Groundwater Quality in Private Domestic Wells: A Case Study from a Temperate Maritime Climate. *J. Hydrol.* **2021**, *601*, 126669. [[CrossRef](#)]
37. Mandel, S.; Shiftam, Z.L.; Hamill, L.; Bell, F.G.; Ingraham, N.L.; Caldwell, E.A.; Verhagen, B.T.; Finkelman, R.B.; Orem, W.H.; Plumlee, G.S.; et al. Sustainability of Morocco's Groundwater Resources in Response to Natural and Anthropogenic Forces. *J. Hydrol.* **2021**, *603*, 106795. [[CrossRef](#)]
38. Ravindra, K.; Thind, P.S.; Mor, S.; Singh, T.; Mor, S. Evaluation of Groundwater Contamination in Chandigarh: Source Identification and Health Risk Assessment. *Environ. Pollut.* **2019**, *255*, 113062. [[CrossRef](#)]
39. Chique, C.; Hynds, P.; Burke, L.P.; Morris, D.; Ryan, M.P.; Dwyer, J.O. Contamination of Domestic Groundwater Systems by Verotoxigenic Escherichia Coli (VTEC), 2003–2019: A Global Scoping Review. *Water Res.* **2021**, *188*, 116496. [[CrossRef](#)]
40. Ferrerons, G.M.; Folch, A.; Masó, G.; Sanchez, S.; Sanchez-Vila, X. What are the main factors influencing the presence of faecal bacteria pollution in groundwater systems in developing countries? *J. Contam. Hydrol.* **2019**, *228*, 103556. [[CrossRef](#)]
41. Ferrer, N.; Folch, A.; Lane, M.; Olago, D.; Odida, J.; Custodio, E. Science of the Total Environment Groundwater Hydrodynamics of an Eastern Africa Coastal Aquifer, in- Cluding La Niña 2016–2017 Drought. *Sci. Total Environ.* **2019**, *661*, 575–597. [[CrossRef](#)]
42. Van Elsas, J.D.; Semenov, A.V.; Costa, R.; Trevors, J.T. Survival of Escherichia Coli in the Environment: Fundamental and Public Health Aspects. *ISME J.* **2011**, *5*, 173–183. [[CrossRef](#)]
43. Yang, Y.; Wu, Y.; Lu, Y.; Shi, M.; Chen, W. Microorganisms and Their Metabolic Activities Affect Seepage through Porous Media in Groundwater Artificial Recharge Systems: A Review. *J. Hydrol.* **2021**, *598*, 126256. [[CrossRef](#)]
44. Osei, F.B.; Boamah, V.E.; Agyare, C.; Abaidoo, R.C. Physicochemical Properties and Microbial Quality of Water Used in Selected Poultry Farms in the Ashanti Region of Ghana. *Open Microbiol. J.* **2019**, *13*, 121–127. [[CrossRef](#)]
45. Kadyampakeni, D.; Appoh, R.; Barron, J.; Boakye-Acheampong, E. Analysis of Water Quality of Selected Irrigation Water Sources in Northern Ghana. *Water Sci. Technol. Water Supply* **2018**, *18*, 1308–1317. [[CrossRef](#)]
46. Jin, D.; Ligaray, M.; Kim, M.; Kim, G.; Lee, G.; Pachepsky, Y.A.; Cha, D.; Hwa, K. Science of the Total Environment Evaluating the in Fl Uence of Climate Change on the Fate and Transport of Fecal Coliform Bacteria Using the Modi Fi Ed SWAT Model. *Sci. Total Environ.* **2019**, *658*, 753–762. [[CrossRef](#)]
47. Reynolds, L.J.; Martin, N.A.; Sala-comorera, L.; Callanan, K.; Doyle, P.; Leary, C.O.; Buggy, P.; Nolan, T.M.; Hare, G.M.P.O.; Sullivan, J.J.O.; et al. Identifying Sources of Faecal Contamination in a Small Urban Stream Catchment: A Multiparametric Approach. *Front. Microbiol.* **2021**, *12*, 661954. [[CrossRef](#)]
48. Alsalah, D.; Al-Jassim, N.; Timraz, K.; Hong, P.Y. Assessing the Groundwater Quality at a Saudi Arabian Agricultural Site and the Occurrence of Opportunistic Pathogens on Irrigated Food Produce. *Int. J. Environ. Res. Public Health* **2015**, *12*, 12391–12411. [[CrossRef](#)]
49. Ferguson, C.; Kay, D. Transport of Microbial Pollution in Catchment Systems. In *Animal Waste, Water Quality and Human Health*; Al Dufour, J.B., Gannon, R.B., Eds.; IWA Publishing, London, UK, 2012; ISBN 9781780401232.
50. Ekarini, F.D.; Rafsanjani, S.; Rahmawati, S.; Asmara, A.A. Groundwater Mapping of Total Coliform Contamination in Sleman, Yogyakarta, Indonesia Groundwater Mapping of Total Coliform Contamination in Sleman, Yogyakarta, Indonesia. *IOP Conf. Ser. Earth Environ. Sci.* **2021**, *933*, 012047. [[CrossRef](#)]
51. Ouedraogo, I.; Defourny, P.; Vanclooster, M. Mapping the Groundwater Vulnerability for Pollution at the Pan African Scale. *Sci. Total Environ.* **2016**, *544*, 939–953. [[CrossRef](#)]
52. Carlson, H.K.; Price, M.N.; Callaghan, M.; Aaring, A.; Chakraborty, R.; Kuehl, J.V.; Arkin, A.P.; Deutschbauer, A.M. The Selective Pressures on the Microbial Community in a Metal- Contaminated Aquifer. *ISME J.* **2018**, *13*, 937–949. [[CrossRef](#)]
53. Carneiro, M.T.; Wasserman, J.C. Critical Evaluation of the Factors Affecting Escherichia Coli Environmental Decay for Outfall Plume Models. *Rev. Ambient. e Agua* **2014**, *9*, 445–458. [[CrossRef](#)]
54. Xue, F.; Tang, J.; Dong, Z.; Shen, D.; Liu, H.; Zhang, X.; Holden, N.M. Tempo-Spatial Controls of Total Coliform and *E. Coli* Contamination in a Subtropical Hilly Agricultural Catchment. *Agric. Water Manag.* **2018**, *200*, 10–18. [[CrossRef](#)]
55. Enuneku, A.A.; Abhulimen, P.I.; Omoregie, P.; Osaro, C.; Okpara, B.; Imoobe, T.O.; Ezemonye, L.I. Heliyon Interactions of Trace Metals with Bacteria and Fungi in Selected Agricultural Soils of Egbema Kingdom, Warri North, Delta State, Nigeria. *Heliyon* **2020**, *6*, e04477. [[CrossRef](#)]
56. Ferreira, M.; Vaz-moreira, I.; Gonzalez-pajuelo, M.; Nunes, O.C.; Manaia, M. Antimicrobial Resistance Patterns in Enterobacteriaceae Isolated from an Urban Wastewater Treatment Plant. *FEMS Microbiol. Ecol.* **2007**, *60*, 166–176. [[CrossRef](#)]
57. Ntube, N.S.; Nyangang, A.J.; Agbor, M.-E.N.; Ayuk, A.R. Trace Element Evaluation of Groundwater in Douala, Cameroon. *OALib* **2022**, *9*, 1–21. [[CrossRef](#)]
58. Rajapaksha, R.M.; Tobor-Kapłon, M.A.; Bååth, E. Metal Toxicity Affects Fungal and Bacterial Activities in Soil Differently. *Appl. Environ. Microbiol.* **2004**, *70*, 2966–2973. [[CrossRef](#)]
59. AdDawadmi\_Gover. Available online: [https://ar.wikipedia.org/wiki/%D9%85%D8%AD%D8%A7%D9%81%D8%B8%D8%A9\\_%D8%A7%D9%84%D8%AF%D9%88%D8%A7%D8%AF%D9%85%D9%8A](https://ar.wikipedia.org/wiki/%D9%85%D8%AD%D8%A7%D9%81%D8%B8%D8%A9_%D8%A7%D9%84%D8%AF%D9%88%D8%A7%D8%AF%D9%85%D9%8A) (accessed on 12 March 2022).
60. SSB Annual Yearbook | General Authority for Statistics. 24 October 2010. Available online: <https://www.stats.gov.sa/en/46> (accessed on 24 October 2022).

61. EL-DIDY, S. Evaluation of The Proposed Drainage Network for Lowering the Groundwater Levels in Al-Dawadmi Town. *J. King Abdulaziz Univ. Environ. Arid L. Agric. Sci.* **1997**, *8*, 111–123. [[CrossRef](#)]
62. Al-Zaidi, A.A.; Elhag, E.A.; Al-Otaibi, S.H.; Baig, M.B. Negative Effects of Pesticides on the Environment and the Farmers Awareness in Saudi Arabia: A Case Study. *J. Anim. Plant Sci.* **2011**, *21*, 605–611.
63. Al Shanti, A. *The Geology and Mineralization of the AdDawadmi District of Saudi Arabia*; Imperial College London: London, UK, 1973.
64. El-Sawy, E.K.; Eldougoug, A.; Gobashy, M. Geological and Geophysical Investigations to Delineate the Subsurface Extension and the Geological Setting of Al Ji'lani Layered Intrusion and Its Mineralization Potentiality, Ad Dawadimi District, Kingdom of Saudi Arabia. *Arab. J. Geosci.* **2018**, *11*, 32. [[CrossRef](#)]
65. Johnson, P.R. *Explanatory Notes to the Map of Proterozoic Geology of Western Saudi Arabia*; Saudi Geological Survey Technical Report SGS-TR-2006-4; Saudi Geological Survey: Jeddah, Saudi Arabia, 2006; 62 p.
66. Timeanddate Climate and Weather Averages in Ad Dawadmi, Saudi Arabia. Available online: <https://www.timeanddate.com/weather/saudi-arabia/dawadmi/climate> (accessed on 12 March 2022).
67. Silva, M.I.; Gonçalves, A.M.L.; Lopes, W.A.; Lima, M.T.V.; Costa, C.T.F.; Paris, M.; Firmino, P.R.A.; De Paula Filho, F.J. Assessment of Groundwater Quality in a Brazilian Semiarid Basin Using an Integration of GIS, Water Quality Index and Multivariate Statistical Techniques. *J. Hydrol.* **2021**, *598*, 126346. [[CrossRef](#)]
68. Quevauviller, P.; Thompson, K.C. *Analytical Methods for Drinking Water*; Wiley: Hoboken, NJ, USA, 2005; ISBN 9780470094938.
69. DPIR. Methodology for the Sampling of Surface Water. *North. Territ. Gov.* **1998**, *11*, 1–11.
70. UGSS. *National Field Manual for the Collection of Water-Quality Data. U.S. Geological Survey Techniques of Water-Resources Investigations*; Book 9; USGS: Reston, VA, USA, 2015.
71. Middleton, K.R. A New Procedure for Rapid Determination of Nitrate and a Study of the Preparation of the Phenol-Sulphonic Acid Reagent. *J. Appl. Chem.* **1958**, *8*, 505–509. [[CrossRef](#)]
72. Ahmed, M.A.; Al Aly, I.M.; Bastaweesy, A.; Gomaa, H.E. Modified Low-Priced Ammonia Diffusion Method for the Analysis of Nitrogen Isotopic Composition of Ammonium and Nitrate in Different Water Matrices. *Egypt. J. Radiat. Sci. Appl.* **2006**, *21*, 257–281.
73. Water Quality-HyServe. Available online: <https://hyserve.com/en/solutions/water-quality/> (accessed on 28 October 2022).
74. Feng, P.C.S.; Hartman, P.A. Fluorogenic Assays for Immediate Confirmation of Escherichia Coli. *Appl. Environ. Microbiol.* **1982**, *43*, 1320–1329. [[CrossRef](#)]
75. Hansen, W.; Yourassowsky, E. Detection of  $\beta$ -Glucuronidase in Lactose-Fermenting Members of the Family Enterobacteriaceae and Its Presence in Bacterial Urine Cultures. *J. Clin. Microbiol.* **1984**, *20*, 1177–1179. [[CrossRef](#)] [[PubMed](#)]
76. Ahmad, A.Y.; Al-Ghouti, M.A.; Khraisheh, M.; Zouari, N. Hydrogeochemical Characterization and Quality Evaluation of Groundwater Suitability for Domestic and Agricultural Uses in the State of Qatar. *Groundw. Sustain. Dev.* **2020**, *11*, 100467. [[CrossRef](#)]
77. Komisarek, J. Groundwater chemistry and hydrogeochemical processes in a soil catena of the poznań Lakeland. *J. Elem.* **2017**, *22*, 681–695. [[CrossRef](#)]
78. Mallick, J.; Singh, C.K.; AlMesfer, M.K.; Kumar, A.; Khan, R.A.; Islam, S.; Rahman, A. Hydro-Geochemical Assessment of Groundwater Quality in Aseer Region, Saudi Arabia. *Water* **2018**, *10*, 1847. [[CrossRef](#)]
79. USEPA. National Primary Drinking Water Regulations | Ground Water and Drinking Water | US EPA. Available online: <https://www.epa.gov/ground-water-and-drinking-water/national-primary-drinking-water-regulations#Inorganic> (accessed on 23 February 2021).
80. WHO. *PH in Drinking-Water Revised Background Document for Development of WHO Guidelines for Drinking-Water Quality*; WHO/SDE/WSH/07.01/1; WHO: Geneva, Switzerland, 2007.
81. USEPA. *National Primary Drinking Water Guidelines*; Epa 816-F-09-004; USEPA: Washington, DC, USA, 2009; Volume 1, p. 7.
82. Gulf Technical Regulation GSO5/DS, D. GCC Standardization Organization (GSO). *Food Packag. Part 2 Plast. Package-Gen. RequirEments* **2013**, *2013*, 83.
83. How Water Activity and PH Synergize | METER Group. Available online: <https://www.metergroup.com/en/meter-food/expertise-library/how-water-activity-and-ph-work-together-control-microbial-growth> (accessed on 25 October 2022).
84. Curtis, T.P.; Mara, D.D.; Silva, S.A. Influence of PH, Oxygen, and Humic Substances on Ability of Sunlight to Damage Fecal Coliforms in Waste Stabilization Pond Water. *Appl. Environ. Microbiol.* **1992**, *58*, 1335–1343. [[CrossRef](#)] [[PubMed](#)]
85. Wahyuni, E.A. The Influence of PH Characteristics on The Occurance of Coliform Bacteria in Madura Strait. *Procedia Environ. Sci.* **2015**, *23*, 130–135. [[CrossRef](#)]
86. Minitab Support System. The Anderson-Darling Statistic-Minitab. Available online: <https://support.minitab.com/en-us/minitab/18/help-and-how-to/statistics/basic-statistics/supporting-topics/normality/the-anderson-darling-statistic/> (accessed on 17 March 2022).
87. Minitab®18 Support Overview of Boxplot-Minitab. Boxplot to Assess and Outliers for Each Group. Available online: <https://support.minitab.com/en-us/minitab/20/help-and-how-to/graphs/boxplot/before-you-start/overview/#:~:{}:text=Use> (accessed on 24 October 2022).
88. Marois-Fise, J.T.; Carabin, A.; Lavoie, A.; Dorea, C.C. Effects of Temperature and PH on Reduction of Bacteria in a Pointof- Use Drinking Water Treatment Product for Emergency Relief. *Appl. Environ. Microbiol.* **2013**, *79*, 2107–2109. [[CrossRef](#)]

89. Hong, H.; Qiu, J.; Liang, Y. Environmental Factors Influencing the Distribution of Total and Fecal Coliform Bacteria in Six Water Storage Reservoirs in the Pearl River Delta Region, China. *J. Environ. Sci.* **2010**, *22*, 663–668. [[CrossRef](#)]
90. Painchaud, J.; Therriault, J. Assessment of Salinity-Related Mortality of Freshwater Bacteria in the Saint Lawrence Estuary. *Appl. Environ. Microbiol.* **1995**, *61*, 205–208. [[CrossRef](#)]
91. Griebler, C.; Lueders, T.; Mu, H.Z. Microbial Biodiversity in Groundwater Ecosystems. *Freshw. Biol.* **2009**, *54*, 649–677. [[CrossRef](#)]
92. Kozhevnikov, P.A.; Verkhovtseva, N.V. Biological properties of soil and ground waters. *Encycl. Life Support Syst.* **2009**, *30*, 169.
93. Yan, N.; Marschner, P.; Cao, W.; Zuo, C.; Qin, W. Influence of Salinity and Water Content on Soil Microorganisms. *Int. Soil Water Conserv. Res.* **2015**, *3*, 316–323. [[CrossRef](#)]
94. Akhavan, S.; Ebrahimi, S.; Navabian, M.; Shabanpour, M.; Mojtahedi, A. Coli and Chloride Significance of Physicochemical Factors in the Transmission of Escherichia Coli and Chloride. *Kerman Univ. Med. Sci.* **2018**, *5*, 115–122. [[CrossRef](#)]
95. Mamilov, A.; Dilly, O.M.; Mamilov, S.; Inubushi, K. Microbial Eco-Physiology of Degrading Aral Sea Wetlands: Consequences for C-Cycling. *Soil Sci. Plant Nutr.* **2004**, *50*, 839–842. [[CrossRef](#)]
96. Willem, J.; Van Herwerden, M.; Schijven, J. Measuring and Modelling Straining of Escherichia Coli in Saturated Porous Media. *J. Contam. Hydrol.* **2007**, *93*, 236–254. [[CrossRef](#)]
97. Dey, U.; Sarkar, S.; Duttagupta, S.; Bhattacharya, A. Influence of Hydrology and Sanitation on Groundwater Coliform Contamination in Some Parts of Western Bengal Basin: Implication to Safe Drinking Water. *Front. Water* **2022**, *4*, 1–15. [[CrossRef](#)]
98. Minitab Support System. A Comparison of the Pearson and Spearman Correlation Methods-Minitab Express. Available online: <https://support.minitab.com/en-us/minitab-express/1/help-and-how-to/modeling-statistics/regression/supporting-topics/basics/a-comparison-of-the-pearson-and-spearman-correlation-methods/> (accessed on 7 April 2022).